Bull. Chem. Soc. Jpn., 72, 1427—1443 (1999)

Accounts

Synthesis and Characteristics of Complex Multicomponent Oxides Prepared by Polymer Complex Method

Masato Kakihana* **and Masahiro Yoshimura†**

Materials and Structures Laboratory, Tokyo Institute of Technology, Nagatsuta 4259, Midori-ku, Yokohama 226-8503

†Center for Materials Design, Materials and Structures Laboratory, Tokyo Institute of Technology, Nagatsuta 4259, Midori-ku, Yokohama 226-8503

(Received January 5, 1999)

This account focuses on the synthesis and characteristics of ceramics prepared by the Pechini-type in-situ polymerizable complex (**IPC**) method. The current status of the **IPC** method is reviewed, and the principle and underlying chemistry of the **IPC** method is illustrated with a special emphasis on its intrinsic advantage over other solution-based technologies. The method has the ability to prepare complex multicomponent oxides with good homogeneity through mixing at the molecular level. The importance of "polymerization" itself in the **IPC** route is demonstrated by comparing with the *non*-polymerizable so-called amorphous citrate method, which affords less compositional homogeneity. The use of heterometallic complexes in the **IPC** processing is shown to be one of the most promising techniques to synthesize ceramics with exceptionally good homogeneity. It is one function of this account to describe how Raman and ^{13}C NMR spectroscopies can be effectively used for characterizing precursors in the **IPC** processing. Finally, it is demonstrated that another type of polymer complex solution (**PCS**) method overcomes the serious drawback of the **IPC** method; i.e. the amount of organics required for the **PCS** method is less than that required for the **IPC** method by a factor of about 20.

Owing to the interdisciplinary nature of ceramics, their chemistry becomes increasingly important especially in the manufacture of ceramic materials with tailored properties. In particular, solution chemistry can play two important roles in further exploitation of processing of ceramics; it will contribute to (1) the low-temperature synthesis of highly pure and homogeneous substances usually in the form of powders, and (2) the development of fabrication techniques for forming useful shapes, e.g. films, fibers and monoliths. Numerous solution techniques have then been developed to synthesize ceramics with improved physical and chemical properties; those including coprecipitation, sol–gel processing of colloids or organo-metallic compounds, hydrothermal processing, spray pyrolysis processes, and gel processing of organic polymers or polymerizable media in the presence of metal complexes.[1—11] All these techniques have their own advantages and disadvantages because of the differences of the chemical principles involved in each technology, and it is beyond the scope of this account to describe each individual characteristic. In this account we focus almost exclusively on gel routes involving formation of organic polymer complexes. In order to elucidate the characteristic of gel processing of organic polymer complexes, we try to classify "gel" technology into several categories as shown in Fig. 1.

A gel is defined as a 3-dimensionally interconnected solid network expanding throughout a fluid medium. Figure 1 is one possible classification of "gel" technology, focusing on the supporting structure of the solid network and its bonding fashion, and the most commonly used source to prepare the solid network. The class (1) differs from the class (2), (3), and (5) in that its interconnected solid network is not made of polymers but colloidal sol particles. The colloidal gel should be discriminated from "precipitate" of solid particles not interconnected. The class (2) is often regarded as the counterpart of the class (1); i.e. it includes instead of colloidal particles an infinite 3-dimensional metal-oxygen inorganic polymer, which is synthesized almost exclusively from metal alkoxides. From this viewpoint, while a gel derived from colloidal sol particles is called "colloidal gel," the one derived through hydrolysis and condensation of metal alkoxides is said to be "polymeric gel."[1] Gels classified as (3) in Fig. 1 are widely used in organic and polymer chemistry, which are not directly connected with the field of inorganic chemistry or ceramic science. It is open to question if "metal-complex" can be regarded as a component forming a solid network in a given "gel" (as (4) in Fig. 1). This is because the distinction between weakly interconnected metal-complexes and a viscous liquid of one continuous phase is rather equiv-

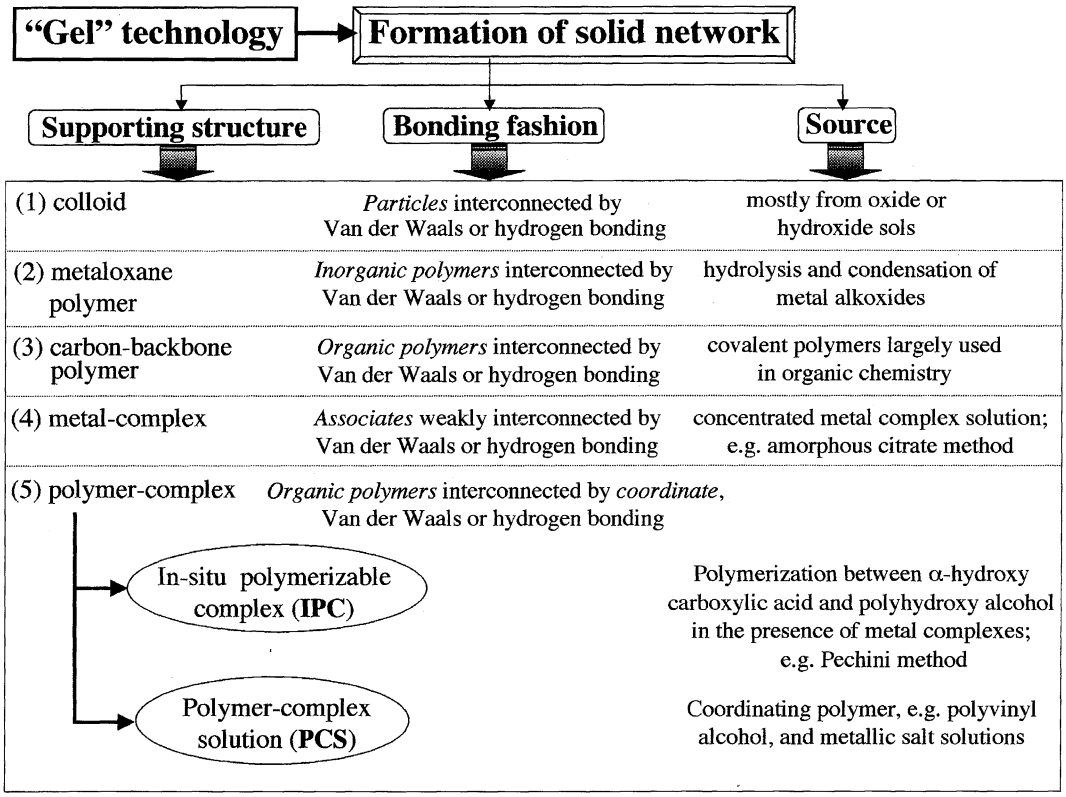

Fig. 1. An example of classification of "gel" technology.

ocal. The amorphous citrate method often called the citrate "gel" method[12] is a case in point. Finally, the class (5), which is the subject of this account, involves no inorganic metal-oxygen polymer but a rigid organic polymer. The organic polymer complex methods can be classified into two categories: i.e. i) a process including "in-situ" polymerization of organics, which we refer to as "In-situ Polymerizable Complex (**IPC**)" method and ii) a process utilizing a coordinating polymer with affinity to metal ions, which we refer conveniently to as "Polymer Complex Solution (**PCS**)" method. The polymer complex method can occupy an unique position in the entire gel technology, as shown in Fig. 1.

One of the characteristic features in the **IPC** method is that it includes a combined process of metal-complex formation and "in-situ" polymerization of organics. A representative example of this approach is the method patented by Pechini in 1967.[13] The patent states formation of a polymeric resin produced through *polyesterification* between metal-complexes using an α-hydroxycarboxylic acid such as citric acid and a polyhydroxy alcohol such as ethylene glycol. The polymeric resin is then calcined to produce the desired oxide. The basic idea behind the Pechini-type **IPC** route is to reduce individualities of different metal ions, which can be achieved by encircling stable metal-complexes with growing polymer nets. Immobilization of metal-complexes in such rigid organic polymer nets can reduce segregations of particular metals, thus ensuring the compositional homogeneity.[10,13–16] This is of vital importance for the synthesis of multicomponent oxides with complicated compositions, since the chemical homogeneity with respect to distribution of cations in an entire system of gel often determines the compositional homogeneity of the final oxide. Indeed sol–gel scientists often suffer from chemical and phase heterogeneities in the derived multicomponent gel, owing to the differential hydrolysis and condensation kinetics in each individual metal compound. It is thus crucial for sol–gel scientists to design a suitable precursor solution which enables formation of a homogeneous multicomponent gel without any phase segregation throughout the processing.

This account is organized in the following manner. In Section 1, the principle and underlying chemistry of the Pechini-type **IPC** method is described with a special emphasis on its intrinsic advantage over the other solution-based technologies. In Section 2, we show some examples in order to demonstrate advantages of the **IPC** method, such as the ability to prepare high-pure and homogeneous multicomponent oxides at reduced temperatures. In Section 3, we stress again the importance of "polymerization" itself in the **IPC** route; it is compared with the *non*-polymerizable amorphous citrate method which affords less compositional homogeneity. Section 4 is devoted to describing how Raman and ^{13}C NMR spectroscopies can be effectively used for characterizing precursors used in the **IPC** processing of $MTiO_3$ (M = Ba, Sr, Pb etc.) and $M_2Ti_2O_7$ (M = La, Nd, Y etc.). In Section 5, we explain the intrinsic disadvantage of the **IPC** technique, and describe how the "Polymer Complex Solution (**PCS**)" method may overcome the drawback of the **IPC** method in some instances. Finally, some conclusions are drawn in

Section 6.

1. Principle of the "In-situ Polymerizable Complex (IPC)" Method

The basic chemistry involved in the **IPC** method is related to the formation of metal complexes as well as the dehydration reaction of an α-hydroxycarboxylic acid and a polyhydroxy alcohol, i.e. esterification. Citric acid (CA) and ethylene glycol (EG) is the couple most widely used in the **IPC** process. Upon heating, CA undergoes esterification with EG to produce a polyester resin throughout, ensuring homogeneous distribution of the constituent metal ions.

Many metal ions other than monovalent cations form very stable chelate complexes with CA, since CA is a polybasic compound having three carboxylic acid groups and one alcoholic group in one molecule. The potential ability of CA to solubilize a wide range of metal ions in a mixed solvent of EG and H_2O is of prime importance, especially for systems involving cations that can be readily hydrolyzed to form insoluble precipitates in the presence of water. For example, the **IPC** method can circumvent the serious problem of preferential precipitation of titanium compounds from aqueous media due to spatial fixation of water-resistant titanium–CA complexes in the polymeric resin. From this reason, a number of titanates with the general formula of $MTiO_3$ or $M_2Ti_2O_7$ have been successfully prepared by the Pechini-type **IPC** method, which will be later shown in Section 4.[17—30]

Esterification of CA (both free CA and complexed CA) then occurs readily in the presence of EG at moderate temperatures (100—150 °C), an example of which is given below:

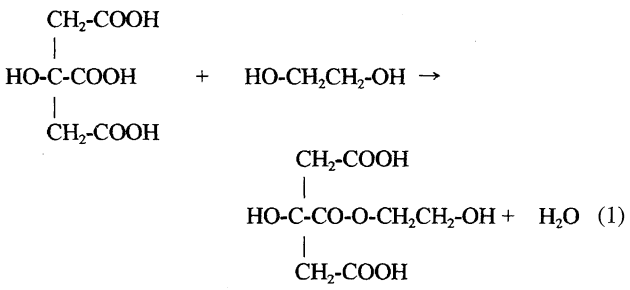

The resulting product of the ester still contains two alcoholic hydroxyl (OH) groups and two carboxylic acid (–COOH) groups, so that it can react further with another CA or EG to form a bigger molecule. This type of reaction occurs in sequence, leading to a polyester resin. As CA has three carboxylic acid groups, branched polyesters may result. Such polyesterifications between CA and EG occurring in the **IPC** process have been indicated indirectly by Anderson et al.[15] and Zhang et al.[31] based on rheological measurements, and more directly by Cho et al.[18] and Kakihana[10] based on infrared and ^{13}C NMR spectroscopy, respectively.

An important aspect of the **IPC** method is that the individual metal CA complexes can be immobilized in a rigid polyester network while preserving the initial stoichiometric ratio of metal ions upon polymerization. The principle of the **IPC** route is thus to obtain a polymeric resin comprising randomly branched polymers, throughout which the cations are uniformly distributed as is schematically shown in Fig. 2. Heating of the polymeric resin at high temperatures (above 300 °C) causes a breakdown of the polymer, and further appropriate heat-treatments yield a fine oxide powder. In spite of the thermoplasticity of the polymer, it is believed that less pronounced segregation of various cations would occur during the pyrolysis because of low cation mobility in such highly crowded branched polymers. In view of this remarkable character,

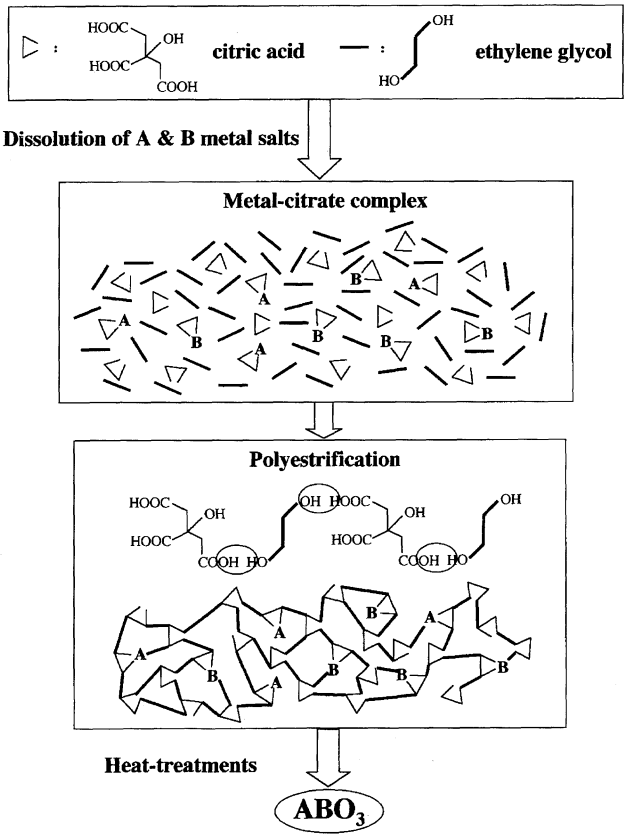

Fig. 2. Concept of the in-situ Pechini-type polymerizable complex (**IPC**) method.

the **IPC** route has an advantage of other solution-based techniques, in particular in the synthesis of complicated multicomponent oxides, where it is crucial to obtain a homogeneous precursor with well interspersed elements for a successful outcome. In fact copper based high-T_c superconductors having extremely complicated compositions were able to be prepared in their pure form by the **IPC** method,[10,31—49] an example of which will be shown in Section 2.3.

2. Highly Pure Nature of Multicomponent Oxides Synthesized by the IPC Method

2.1 Synthesis of Multicomponent Oxides at Reduced Temperatures. The **IPC** method was first developed by Pechini in 1967 to prepare capacitor materials focusing only on niobates, titanates and zirconates.[13] After Pechini the method has been extensively applied towards the synthesis of a variety of multicomponent oxides, such as lead magnesium niobates,[15] $LaMnO_3$,[14,16,50] $LaAlO_3$,[51] Sr-doped lanthanum chromite,[52] Y_3NbO_7,[53] $LiTaO_3$,[54] $K_2La_2Ti_3O_{10}$,[55,56] ZrO_2/CeO_2,[57] ZrO_2/Y_2O_3,[58] ZrO_2/Y_6WO_{12},[59,60] $BaSnO_3$,[61] $BaTi_4O_9$,[62,63] $KTiNbO_5$,[64] $SrTiO_3$,[17—22] $BaTiO_3$,[23—27] $PbTiO_3$,[28] $La_2Ti_2O_7$,[30] $Y_2Ti_2O_7$,[29] and cuprates.[31—49] All the studies previously reported have clearly indicated that the **IPC** method is quite suitable for producing highly pure and homogeneous oxides at reduced temperatures (400—900 °C). Since cations stabilized with CA can be immobilized in a rigid polyester network, the resulting polymeric resin may have the same metal stoichiometry, probably at molecular level, as that of the final multicomponent oxides. It is thus inferred from this viewpoint that, upon the decomposition of the resin at 300—400 °C followed by the calcination at typically 400—900 °C, the contiguous metal ions in a polyester resin or its pyrolyzed product can react with each other with a minimum of

diffusion. Low firing temperatures are then required for synthesizing a phase pure multicomponent oxide, for example 700 °C for $LaAlO_3$ compared to 1700 °C for the conventional solid-state reaction technique, as shown in Fig. 3.[51]

2.2 Possible Molecular-Scale Mixing of Cations in Precursors. We have claimed that success in lowering the crystallization temperature may indicate a dramatically improved level of mixing of cations in both resins and their pyrolyzed products (i.e. precursors for the target oxide).[10,22,27,28,51,53,63] For example no significant segregation of the constituent metals has been observed in the pyrolyzed product of the polymeric resin in the **IPC** synthesis of $SrTiO_3$.[22] The sample of $SrTiO_3$ was prepared by the **IPC** method according to the flow chart of Fig. 4.[22] The decomposition product of the polymeric resin at 350 °C (i.e. the powder precursor in Fig. 4) gave no sharp peaks in its X-ray diffraction (XRD) spectrum, indicating absence of any crystalline intermediates (Fig. 5(a)).[22] $SrTiO_3$ crystallized in its pure form when the pyrolyzed product was further heat-treated at 500 °C (see Fig. 5(c)).[22] A matter of very important concern is then to know whether $SrCO_3$ and TiO_2 are distinct intermediate phases formed prior to the formation of $SrTiO_3$ during the thermal decomposition of the polymeric resin. This is because isolation of $SrCO_3$ and TiO_2 in significant amounts indicates a given Sr–Ti polymeric resin to be compositionally inhomogeneous. The unlikelihood of formation of free $SrCO_3$ and TiO_2 during the thermal decomposition of the Sr–Ti polymeric resin is supported by XRD measurements. As shown in Fig. 6(c),[22] after heat-treating the Sr–Ti polymeric resin in air at 400 °C for 2 h, the XRD pattern of the pyrolyzed product exhibits no reflections from crystalline $SrCO_3$ and TiO_2, instead of which a very broad peak centered at approximately 30° is observed. In contrast with the Sr–Ti polymeric resin, the XRD patterns of products obtained from similar thermal decomposition of polymeric resins containing only Ti or Sr at 400 °C for 2 h exhibit clear reflections from TiO_2 or $SrCO_3$ (Figs. 6(a) and 6(b)).[22] However, it should be noticed that crystallites of dimensions less than about 100 nm give rise to line broadening of XRD, which deteriorates the ability of the XRD technique to detect possible intermediates, in this case TiO_2 or $SrCO_3$. The powders used for the XRD analysis were therefore further characterized using Raman

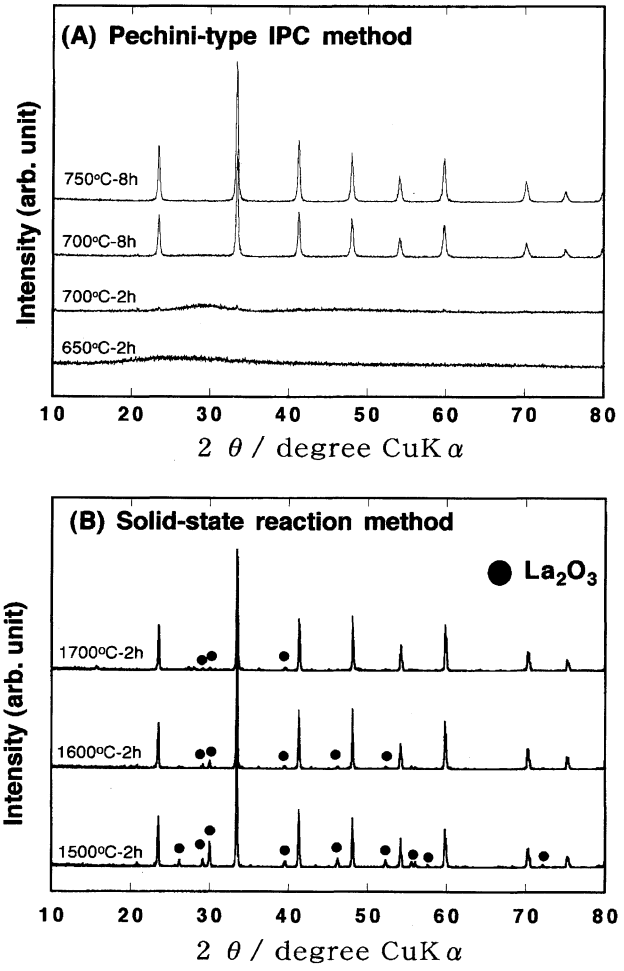

Fig. 3. X-Ray diffraction patterns of products obtained by calcining the **IPC**-derived powder precursor for $LaAlO_3$ (A) and those obtained by the conventional solid-state reactions between La_2O_3 and Al_2O_3 (B) at various temperatures.[51]

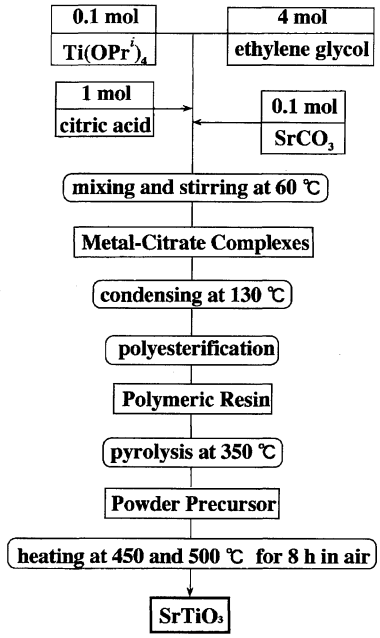

Fig. 4. Flow chart for preparing $SrTiO_3$ by the **IPC** method. The molar ratio of Ti(OPr^i)$_4$/$SrCO_3$/CA/EG = 0.1/0.1/1/4.[22]

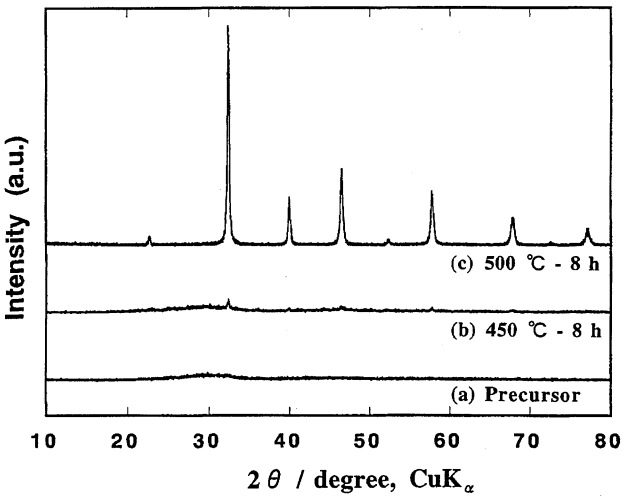

Fig. 5. X-Ray diffraction patterns of the **IPC**-derived powder precursor for $SrTiO_3$ (a) and of samples heat-treated in static air at 450 °C for 8 h (b) and 500 °C for 8 h (c).[22]

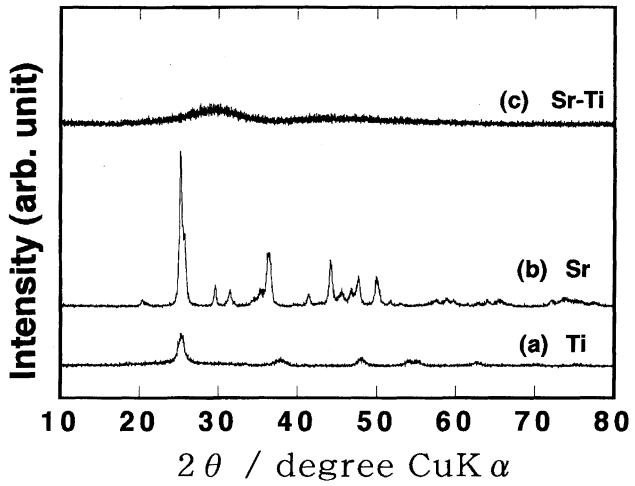

Fig. 6. X-Ray diffraction patterns of products obtained by calcining the **IPC**-derived powder precursors in static air at 400 °C for 2 h: (a) Ti, (b) Sr, and (c) Sr–Ti.[22]

spectroscopy, a technique which is capable of detecting impurities consisting of very small crystallites not easily identified with the XRD technique because of their diffuse reflections. More specifically, it is known that Raman spectroscopy is extremely sensitive to the presence of TiO_2.[65]

Figure 7(b) shows a typical Raman spectrum of a product obtained from the thermal decomposition of a polymeric resin containing both Sr and Ti at 400 °C for 2 h.[22] A characteristic broad band ranging from 1200 to 1700 cm^{-1} is probably attributed to the residual carbon due to the imperfect elimination of organics from the polymeric resin at 400 °C, but it should be noticed that no crystalline TiO_2 was detected by Raman spectroscopy for the Sr–Ti polymeric resin calcined at 400 °C, particularly as evidenced by the complete absence of the strongest anatase Raman peak at 147 cm^{-1} (see the typical Raman spectrum of TiO_2 shown in Fig. 7(a)).[22] Only an assumption that a completely amorphous or a highly defective TiO_2 phase forms exclusively from the Sr–Ti polymeric resin can explain the fact that it is not detected by both XRD and Raman spectroscopy. The possibility for this is low as the corresponding Raman spectrum (Fig. 7(a)) of a product obtained from the thermal decomposition of a polymeric resin containing only Ti at 400 °C for 2 h clearly indicates the presence of crystalline anatase TiO_2.[66] We thus presume that several tens or even nanometer scale mixing of cations has been achieved in the Sr–Ti polymeric resin, which resulted in lowering the $SrTiO_3$ formation temperature from ca. 1000 °C for the conventional solid-state reaction method to ca. 500 °C.

2.3 Improved Material Properties. Ceramics prepared by different techniques often exhibit different properties even with the same overall composition, reflecting small differences in phase purity and compositional homogeneity. Compositional heterogeneity is undesirable, especially in electrical and magnetic ceramics ranging from fully insulating dielectrics to high temperature oxide superconductors. The **IPC** method has an advantage of the conventional solid-state reaction technique with respect to chemical homogeneity and compositional control. Because of this unique character, the **IPC** technique has to be considered as one of preferable means in improving the function of ceramics by a doping technique, for which a uniform distribution of the dopant through the lattice is strictly required. Improved materials properties and performance can, therefore, be expected when the target compound is synthesized by the **IPC** method. An example of this concern is shown in Fig. 8, where the superconducting transition behavior is compared for two polycrystalline samples with the same chemical form of $Bi_2Sr_2Ca_{0.8}Y_{0.2}Cu_2O_{8.2}$ but prepared by different methods.[42] While the first sample prepared by the **IPC** method exhibits a sharp superconducting transition without any discontinuity during the transition, the second sample prepared by the conventional solid-state reaction method exhibits a broad transition; the diamagnetic signal being not saturated even down to 10 K. It is generally acceptable that broadening of the superconducting transition (or transition with discontinuity) reflects the presence of impurity phases and inhomogeneities of the compound.[10] The narrow and smooth superconducting transition of the **IPC**-derived sample is therefore attributable to the high purity and compositional uniformity of the sample prepared by the **IPC** technique.

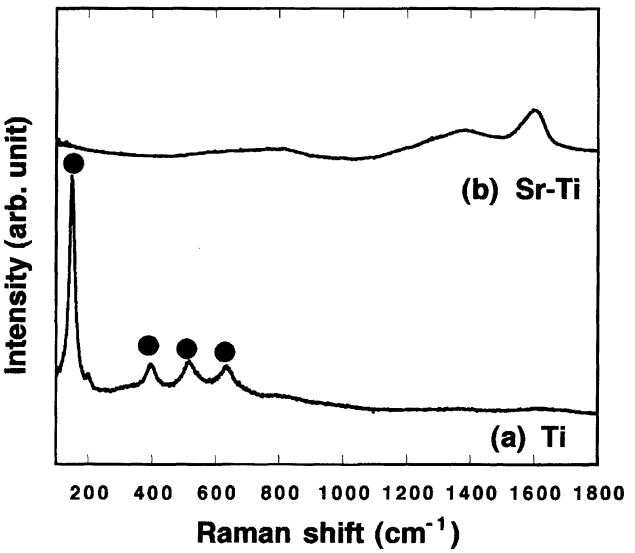

Fig. 7. Raman spectra of products obtained from thermal decomposition of **IPC**-derived powder precursors containing only Ti (a) and both Sr and Ti (b) in static air at 400 °C for 2 h. ● denotes peaks corresponding to anatase TiO_2.[22]

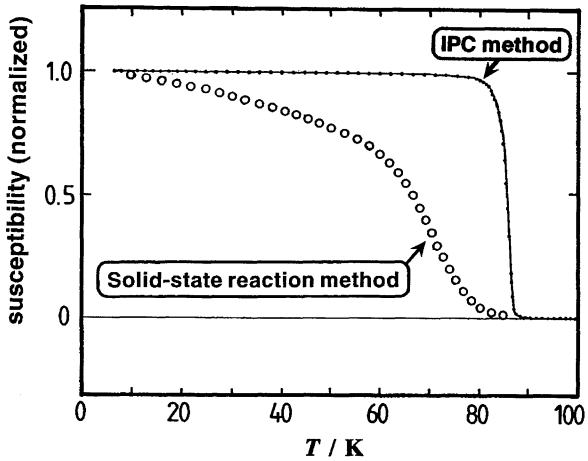

Fig. 8. Real parts of complex magnetic susceptibility for $Bi_2Sr_2Ca_{0.8}Y_{0.2}Cu_2O_{8.2}$ prepared by the **IPC** method (•) and by the conventional solid-state reaction method (○).[42]

3. Importance of Polymerization in the IPC Route—Comparison with Non-polymerizable Amorphous Citrate Method

The literature often is confusing concerning the distinction between the Pechini-type **IPC** method and the amorphous citrate (or other carboxylates such as malate, acetate etc.) method. The amorphous citrate method differs from the Pechini-type **IPC** method in that ethylene glycol (EG) in the **IPC** method is replaced by water. While the **IPC** method involves formation of rigid organic polymeric nets resulting from polyesterification between citric acid (CA) and EG, the amorphous citrate method involves no such polyesterification, but rather formation of weak hydrogen-bonded-like associates (see Fig. 1).[10] It is then expected that a better chemical homogeneity will be achieved in the **IPC** method than the amorphous citrate method, since immobilization of metal–CA complexes in a rigid polyester net can minimize segregations of particular metals during the decomposition process of the polymer at high temperatures.[10] In what follows, we demonstrate the importance of such a polymerization for the synthesis of pure $BaTi_4O_9$ at reduced temperatures as an example.

3.1 $BaTi_4O_9$ from Non-polymerizable Amorphous CA Method. One of the common problems in the synthesis of $BaTi_4O_9$ by alkoxide routes is the difficulty in controlling the rapid hydrolysis of titanium alkoxides (chemicals most frequently used as sources of Ti) compared with barium species. For instance, in the previously reported sol–gel synthesis of $BaTi_4O_9$,[67] gels derived from barium and titanium alkoxide precursors have produced strongly multiphase samples even after the heat-treatment at 1200 °C. The preferential hydrolysis of titanium alkoxides can form Ti-rich clusters, which destroys the cation composition of the original solution. This result tells us that titanium alkoxides should be modified by certain organic compounds such as citric acid or acetic acid to control the degree of hydrolysis and subsequent polycondensation reactions.[10,68—70] Alternatively, Choy et al. attempted to synthesize $BaTi_4O_9$ at lower temperatures by the amorphous citrate technique.[71] However, the citrate-derived precursor produced strongly multiphase samples with sizable amounts of Ti-rich barium titanates such as $BaTi_5O_{11}$ and $Ba_2Ti_9O_{20}$ after the heat-treatment at temperatures below 900 °C. Firing the precursor at 1300 °C was required to obtain phase pure $BaTi_4O_9$.

A similar result has been observed in the **IPC**-based synthesis of $BaTi_4O_9$ in our laboratory, when the polymerization is intentionally suppressed by increasing the pH of the solution using ammonia. An interesting comparison can then be made as to the phase evolution of $BaTi_4O_9$ between the original Ba/Ti = 1/4 CA–EG solution (pH≈0.1) and the one modified by ammonia (pH≈3). Figure 9 shows XRD patterns of the amorphous precursor (derived from the high-pH solution) calcined in air at different temperatures for 2 h. As is clearly seen, no phase pure $BaTi_4O_9$ could be obtained even after calcination at 1200 °C. Formation of $BaTi_5O_{11}$ in preference to $BaTi_4O_9$ at temperatures below 800 °C may imply that a –Ti–O–Ti– network is built up around a barium ion, thus creating clusters locally rich in Ti with respect to Ba. An important concern is that the addition of ammonia plays a role not only to promote the preferential hydrolysis of $Ti(OPr^i)_4$ but also to inhibit ester reactions between CA and EG. The inhibition of ester reactions by ammonia comes from an increased pH of the solution that significantly enhances the dissociation of protons from carboxylic acid (–COOH) groups in CA according to the following type of reaction:

$$R(COOH)_3 + nOH^- \rightarrow R(COOH)_{3-n}(COO^-)_n + nH_2O \quad (2)$$

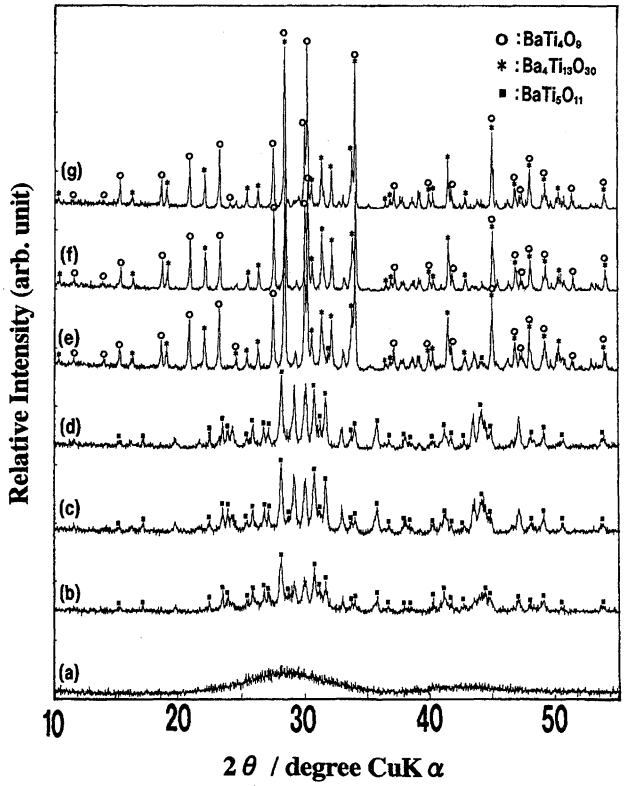

Fig. 9. X-Ray diffraction patterns of the **IPC**-derived powder precursor (derived from an ammonia containing solution (pH = 3)) for $BaTi_4O_9$ calcined in static air for 2 h at 600 °C (a), 650 °C (b), 700 °C (c), 800 °C (d), 900 °C (e), 1000 °C (f), and 1200 °C (g). No single-phase of $BaTi_4O_9$ has been obtained even after the heat-treatment at 1200 °C.

where $R(COOH)_3$ stands for CA with an emphasis of its tribasic nature. Ester reactions occur only between carboxylic acid (–COOH) groups of CA and hydroxyl (–OH) groups of EG (see Eq. 1), while the dissociated carboxylate ($–COO^-$) groups do not participate in the esterification. Thus an increased fraction of COO^- in CA due to an increase in pH renders the solution fluid or non-viscous; that ruins one of the most characteristic features of the **IPC** method based upon polyesterification. Molecular-scale mixing of the original solution is no longer maintained in this case, because the lower the viscosity of the solution, $Ti(OPr^i)_4$ has the more chance of forming Ti-rich clusters as a result of its preferential hydrolysis.

3.2 $BaTi_4O_9$ from the IPC Method.[62,63] In sharp contrast to the case described in Section 3.1, a rigid polyester network easily forms starting from the original solution nonmodified by ammonia. The pH of the original solution is ca. 0.1, which indicates that most of CA remain undissociated, thus favoring polyesterification between CA and EG. It is probable that prior to the occurrence of hydrolysis of Ti-species, metal species are frozen in a rigid polyester network while preserving the cation composition identical to that of the original solution. Molecular-level mixing is now maintained better in this case, as is demonstrated by the successful synthesis of $BaTi_4O_9$ at 700—900 °C.[62,63]

The XRD patterns of powders obtained after calcining the amorphous precursor (derived from the low-pH solution) in air at three different temperatures for 2 h are shown in Fig. 10 in 2θ range of 10—55°.[63] The **IPC**-derived precursor fired at 650 °C was primarily amorphous in structure, as shown by the broad continuum in the XRD in Fig. 10(a). Substantial crystallization occurred during the

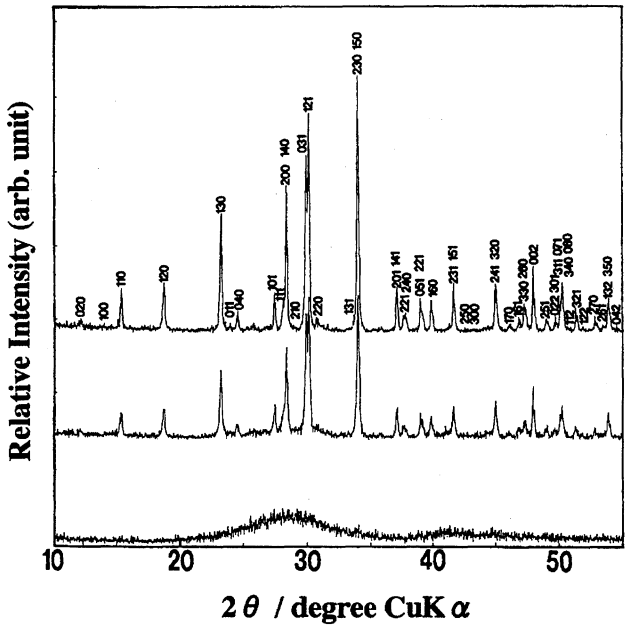

Fig. 10. X-Ray diffraction patterns of the **IPC**-derived powder precursor (derived from the original solution nonmodified by ammonia) for $BaTi_4O_9$ calcined in static air for 2 h at 650 °C (a), 700 °C (b), and 800 °C (c).[62]

heat treatment of the **IPC**-derived precursor in air at 700 °C for 2 h (Fig. 10(b)). All the well-defined peaks in the XRD patterns of Figs. 10(b) and 10(c) exhibited a pure orthorhombic phase of $BaTi_4O_9$ in good agreement with the diffraction pattern observed for this compound by Phule et al.[72] It should be stressed here that the impurity phases $BaTi_5O_{11}$, $Ba_2Ti_9O_{20}$, $Ba_4Ti_{13}O_{30}$, and $BaTi_2O_5$, which are most frequently formed as by-products during the synthesis of $BaTi_4O_9$, were not detected by XRD. Another important aspect worthwhile mentioning is that no reflections from $BaCO_3$ and TiO_2 were observed as distinct intermediate phases prior to the formation of $BaTi_4O_9$ during the thermal decomposition of the **IPC**-derived precursor at 650 °C. Since it is known that well-crystalline $BaCO_3$ and TiO_2 are obtained at 400—500 °C from similar thermal decompositions of powder precursors containing only Ba or Ti,[27,73] no detection of $BaCO_3$ and TiO_2 from the Ba/Ti = 1/4 composition precursor should be considered as an implication of almost perfect mixing of the constituent cations in the powder precursor, as in the case of $SrTiO_3$ mentioned in 2.2.

Lowering the synthetic temperature is of practical importance when the powder is used as a catalytic material. This is because the catalytic activity is generally decreased with an increase in the synthetic temperature as a consequence of reduction of the specific surface area. $BaTi_4O_9$, when combined with RuO_2, can be used as a photocatalyst for water decomposition that has recently emerged as a new class of materials.[74—78] In fact, a $RuO_2/BaTi_4O_9$ material prepared by the **IPC** method at 800 °C showed a photocatalytic activity ca. 5 times higher than that of a material prepared by the conventional solid-state reaction technique at 1100 °C.[63]

4. Spectroscopic Characterization of Precursors for Ceramics

4.1 Heterometallic Alkoxides as Precursors. A basic understanding of the precursor solution chemistry by means of appropriate spectroscopic techniques is a useful approach for the subsequent establishment of optimum preparative conditions and thus could allow a better control of the properties of the resulting oxide material.[7,79] One wants to design a precursor solution that forms a heterometallic complex with exactly the same metal stoichiometry as that of the desired oxide product. A so-called double alkoxide with the form of e.g. $AB(OR)_n$ is a case in point. It is plausible that such a heterometallic alkoxide may be hydrolyzed with a controlled amount of water, as if it were a single molecule rather than the individual alkoxide mixture, thereby favoring the molecular-level formation of mixed-metal oxygen bonds of –A–O–B– between the two metals. Subsequent polymerization may yield a multicomponent gel having the same metal stoichiometry as the initial double alkoxide molecule. This character of the heterometallic alkoxide may circumvent the mismatch of the hydrolysis and condensation rates of its individual component metal alkoxides, thus resulting in the need to convert the gel to the desired oxide at reduced temperatures. Spectroscopic techniques such as IR (infrared), Raman, NMR (nuclear magnetic resonance), and mass spectroscopies play an important role in identifying such a heterometallic complex in solution and in studying the chemistry behind a series of hydrolysis and condensation reactions, thus possibly leading us to a useful solution precursor for a target oxide. A summary of available heterometallic alkoxides was provided by Mehrotra,[80] and extensive reviews on the synthesis, structures and reactivity of heterometallic alkoxides were given by Caulton and Hubert–Pfalzgraf[79] and Chandler, Roger and Hampden–Smith.[7]

A well-known example of a heterometallic alkoxide useful as a precursor is $LiNb(OEt)_6$. This complex is synthesized simply by refluxing an ethanol solution of Li(OEt) and $Nb(OEt)_5$ with Li/Nb ratio of 1.[81] NMR spectroscopic evidence for the formation, in solution, of the heterometallic lithium niobium ethoxide was presented by Eichorst et al.,[82] and the compound $LiNb(OEt)_6$ isolated from the solution was investigated in the solid-state by single-crystal X-ray diffraction, where the structure was characterized by the presence of infinite helical polymers of niobium octahedra cis linked by severely distorted tetrahedral lithium atoms.[83] Solutions of this compound have been hydrolyzed to form high-quality $LiNbO_3$ films and powders at reduced temperatures (250—400 °C).[84—88] It has been demonstrated from ^{93}Nb and ^{7}Li NMR spectroscopy that additions of acid (HNO_3) or base (NH_3 aq) catalyst result in significant changes in the niobium environment owing to different polycondensation mechanisms, while the lithium environment remained relatively unaffected irrespective of catalyst.[82] Different network structures may form depending upon the catalyst used, which would lead to differences in the crystallization behavior of catalyzed gels resulting from different rearrangement processes. Indeed, acid-catalyzed gels crystallized approximately 20 °C lower than base-catalyzed samples; this was attributed to variations in gel structure and rearrangement processes.[82,89] An important conclusion drawn from this study is that solution chemistry has an effect on the evolution of structure in the sol–gel processing of lithium niobate.[82]

It should, however, be mentioned here that the tendency towards disproportionation during hydrolysis is a major problem in the sol–gel processing using heterometallic alkoxides.[90] For instance, hydrolysis of $BaTi(OCH_2CH_2OCH_3)_6$, obtained via a reaction of $Ba(OCH_2CH_2OCH_3)_2$ and $Ti(OCH_2CH_2OCH_3)_4$ in 2-methoxyethanol,[91] with 1 equivalent of water per alkoxide ligand gave the oxo species $Ba_4Ti_{13}O_{18}(OCH_2CH_2OCH_3)_{24}$, although addition of an excess of water to a solution of $BaTi(OCH_2CH_2OCH_3)_6$ afforded powders of perovskite $BaTiO_3$ at a temperature as low as 400 °C[91] and afforded thin films at 600—700 °C.[92] The new oxo Ba : Ti = 4 : 13 heterometallic alkoxide isolated from a $BaTi(OCH_2CH_2OCH_3)_6$ solution partially hydrolyzed was then utilized as a precursor for $Ba_4Ti_{13}O_{30}$,[91] a material finding applications in high-frequency resonators.[93]

4.2 Heterometallic Citrates in the IPC Method. Disproportionation of heterometallic alkoxides upon hydrolysis, which is often encountered in the sol–gel processing, may be greatly suppressed in the Pechini-type **IPC** processing. This is not surprising because the **IPC** method involves a step of the spatial separation of each individual metal complexes at a molecular level in a highly viscous resin (see Fig. 2). The maximum chemical homogeneity may be achieved in the **IPC** processing when a heterometallic complex with a desired stoichiometry is utilized rather than the individual component metal complexes. Our expectation is then that this type of heterometallic complex can be frozen in a polyester-type resin without significant change in the correct cationic stoichiometry, when the polymerization is carried out under mild conditions. According to this strategy, heterometallic citrates with a desired stoichiometry were designed as successful precursors for the synthesis of $MTiO_3$ (M = Ba, Sr, Pb)[22,26—28] and $Ln_2Ti_2O_7$ (Ln = Y and rare-earth elements)[29,30] by the **IPC** method. In what follows, we describe results of the spectroscopic characterization of the Ba–Ti–CA–EG–(H_2O) system, which has been used as a precursor solution for the low temperature synthesis of $BaTiO_3$.[23—27,94]

(4.2.1) Evidence for Formation of a Heterometallic BaTi–CA_3 Complex.[27,94] We have indicated in previous publications[27,94] that Ba^{2+} and Ti^{4+} ions individually complexed with CA in CA/EG solutions react to form a stable Ba : Ti = 1 : 1 heterometallic CA complex according to the following type of reaction (the charge for each chemical species is omitted for simplicity):

$$a\mathrm{Ba} + a\mathrm{Ti} + b\mathrm{CA} \rightarrow a[\mathrm{BaTi\text{–}CA}_n] + (b - an)\mathrm{CA} \qquad (3)$$

Strong evidence for formation of a heterometallic complex with a stoichiometry close to Ba : Ti : CA = 1 : 1 : 3 (i.e. BaTi–CA_3) has been obtained from an extensive Raman and ^{13}C NMR spectroscopic study on many CA/EG solutions with various amounts of Ba and Ti ions.[94]

Figure 11 shows Raman spectra of CA/EG solutions without metal ions (a), containing Ba ions (b), Ti ions (c) and both Ba and Ti ions (d).[27,94] An important observation here is that the Raman spectrum of BaTi-CA/EG cannot be interpreted in terms of a simple superposition of the individual Ba–CA/EG and Ti–CA/EG Raman spectra. The simultaneous presence of barium and titanium cations in CA/EG solution has induced substantial changes in the ν(C=O) Raman band near the 1730 cm^{-1} region[95,96] and the ν(Ti–O) Raman band near the 600 cm^{-1} region,[97] where ν(C=O) and ν(Ti–O) denote the carbonyl and Ti–O stretching vibrations, respectively. This suggests that barium and titanium cations have a strong interaction during the chelation, to form a heterometallic CA complex. A more substantial conclusion can be drawn from the ^{13}C NMR spectra of these solutions, the results of which are shown below.[27,94]

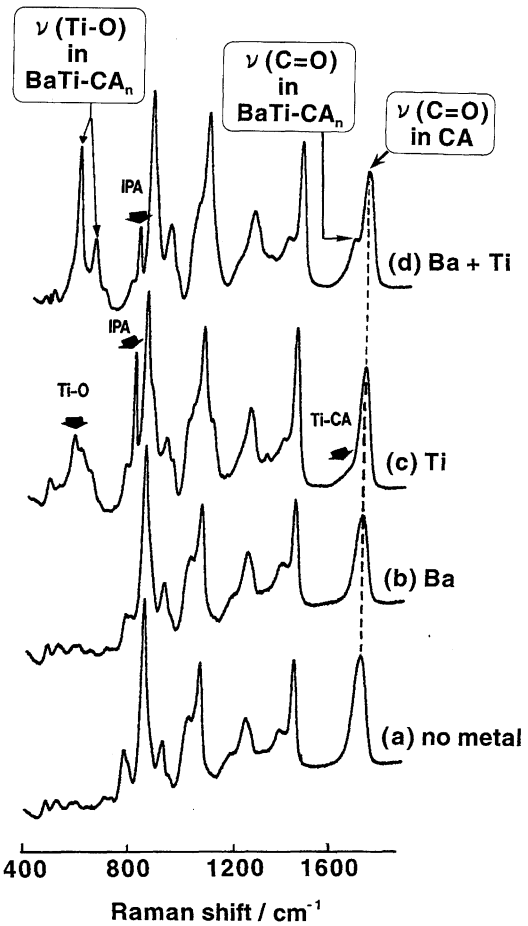

Fig. 11. Raman spectra of various solutions with the molar ratio Ba : Ti : CA : EG = (a) 0 : 0 : 1 : 4, (b) 0.2 : 0 : 1 : 4, (c) 0 : 0.2 : 1 : 4, and (d) 0.2 : 0.2 : 1 : 4.[27,94] ν(C=O) and ν(Ti–O) denote the carbonyl and Ti–O stretching vibrations, respectively.

Figure 12 shows a selected region of $^{13}C\{^1H\}$ NMR (decoupled) spectra of CA/EG solutions without metal ions (a), containing Ba ions (b), Ti ions (c) and both Ba and Ti ions (d).[27,94] Resonance signals marked with ○ are due to methylene carbons (46 ppm) in CA,[98] and they are used as internal standards for estimation of integrated intensities in different samples. A numerous number of resonances in a 60—74 ppm region (◆) correspond to methylene carbons in unreacted EG[98] or those in a variety of esterificated EG species. In what follows we concentrate our attention on a

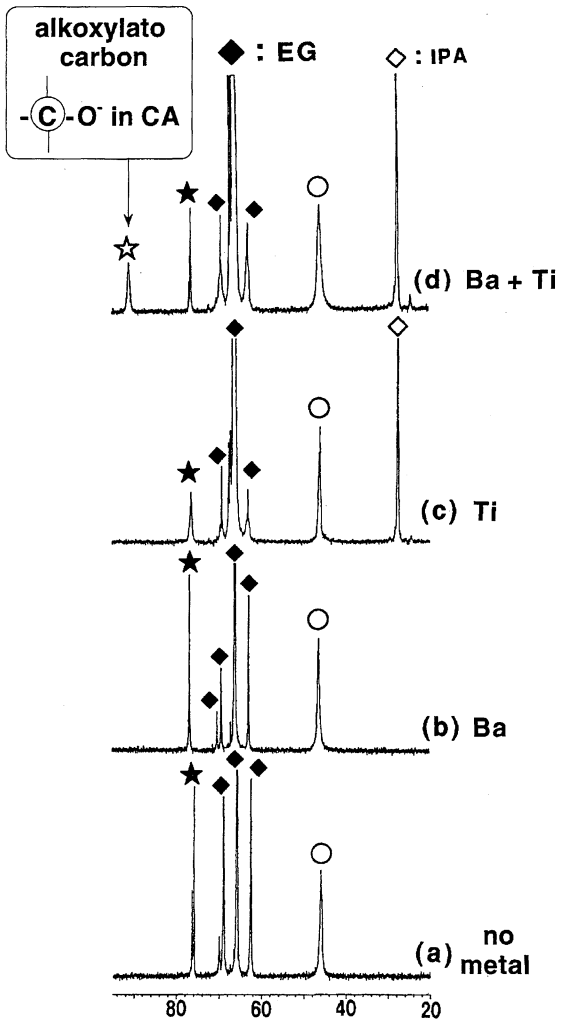

Fig. 12. $^{13}C\{H\}$ NMR (decoupled) spectra in a region of 20—95 ppm for various solutions with the molar ratio Ba : Ti : CA : EG = (a) 0 : 0 : 1 : 4, (b) 0.2 : 0 : 1 : 4, (c) 0 : 0.2 : 1 : 4, and (d) 0.2 : 0.2 : 1 : 4. IPA stands for isopropyl alcohol. For definition of other symbols marked on peaks, see text.[27,94]

74—95 ppm region, where resonances associated with alcoholic carbons (78 ppm) in CA (or in CA esterificated with EG) occur,[98] the position of which is marked with ★.

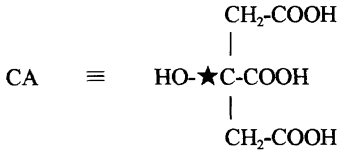

(4)

A striking result is that the simultaneous presence of Ba and Ti ions in the CA/EG solution gives rise to a new resonance at 91 ppm (marked with ☆) in addition to the resonances at 78 ppm (marked with ★) associated with the alcoholic carbon of CA (Fig. 12(d)), which in turn indicates that the molecular constitution of the BaTi–CA/EG solution cannot be described as a simple combination of those characteristic for the individual Ba–CA/EG and Ti–CA/EG solutions in accordance with the Raman spectroscopic data (see Fig. 11). From off-resonance ^{13}C NMR experiments, the origin of the 91 ppm peak has been unambiguously assigned to the corresponding quaternary carbon in CA with dissociation of a proton from the alcohol OH group, i.e. the alkoxylato-carbon (☆) as described in Eq. 5:

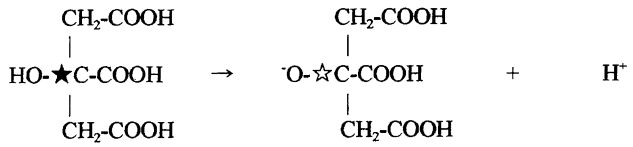

(5)

Since the ionization described by Eq. 5 is never expected in solutions free from metals even at very high pH,[99—101] the alkoxylato –C–O$^-$ group responsible for the resonance at 91 ppm in Fig. 12(d) should be present not as a free ion but as a ligand stabilized through complexation. Intensities for the peak at 91 ppm can then be used as a measure of the concentration of the heterometallic complex unique to BaTi–CA/EG solutions. Indeed, the relative intensities of the 91 ppm signal were found to linearly increase with increasing the amount of Ba (= c(Ba)), while the amount of Ti (= c(Ti)) is set to equal to c(Ba), which was accompanied with a linearly decreased intensity of the 78 ppm peak (Fig. 13).[27,94] This observation indicates that the peak at 91 ppm is attributable to the alkoxylato-CA in a given BaTi–CA$_n$ complex unique to the BaTi–CA/EG solution, while the 78 ppm feature is attributable mostly to excess free CA (or CA esterificated with EG). The fact that addition of either Ba or Ti in excess (deviating from a ratio of Ba/Ti = 1) gave rise to no substantial change in the relative intensities of the 91 ppm peak supports our proposition that the simultaneous presence of Ba and Ti ions in CA/EG solutions produces a heterometallic BaTi–CA$_n$ complex with a stoichiometric Ba/Ti = 1 ratio.[94]

The value of n in BaTi–CA$_n$ can be evaluated from a plot giving a relationship between c(Ba) (the known amount of Ba) and c(Alk) (the amount of alkoxylato-CA). Values of c(Alk) were calculated from the total amount of CA and the values of $I(91)/(I(78)+I(91))$ experimentally determined from the ^{13}C NMR spectra shown in Fig. 13, where I(91) and I(78) represent the respective integrated intensities of the 91 ppm signal (corresponding to the alkoxylato-CA) and of the 78 ppm signal (corresponding to free nonalkoxylato-CA). When the complexation follows Eq. 3, c(Alk) and c(CA) (the amount of nonalkoxylato-CA) should be, respectively, increased and decreased with increasing c(Ba) (i.e. "a" in Eq. 3), while keeping the total amount of CA (i.e. "b" in Eq. 3) constant. This has indeed been observed, as shown in Fig. 14.[27,94] A linear increase of c(Alk) with c(Ba), which is accompanied with a linearly decreased c(CA), thus indicates that the amount of the heterometallic BaTi–CA$_n$ is linearly increased at the expense of free CA. The extrapolation of the linear c(Alk) vs c(Ba) plot to c(Ba) = 1 mol gives the amount of CA participating in the formation of the heterometallic BaTi–CA$_n$, and one can now have $n \fallingdotseq 3$.[27,94]

(4.2.2) A Model Structure of BaTi–CA$_3$ Complex.[94]

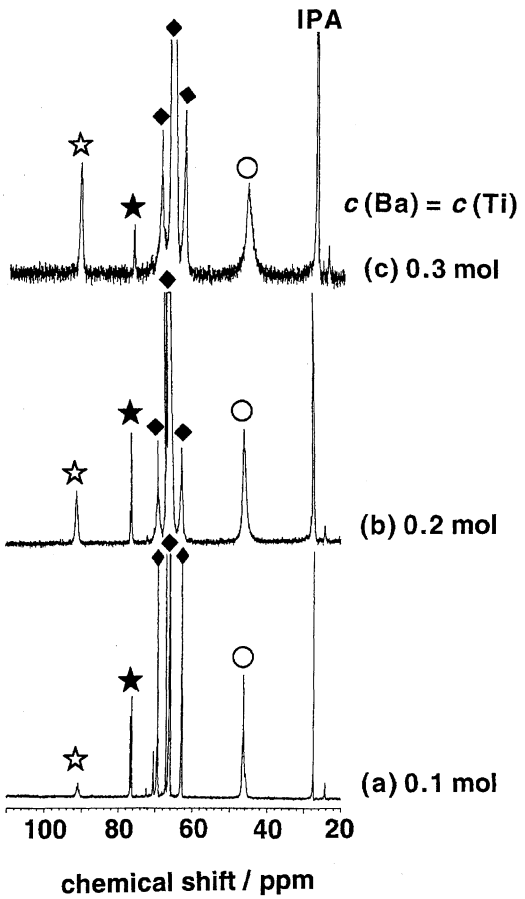

Fig. 13. $^{13}C\{H\}$ NMR (decoupled) spectra in a region of 20—110 ppm for various solutions with the molar ratio Ba : Ti : CA : EG = (a) 0.1 : 0.1 : 1 : 4, (b) 0.2 : 0.2 : 1 : 4, and (c) 0.3 : 0.3 : 1 : 4. IPA stands for isopropyl alcohol. For definition of other symbols marked on peaks, see text.[27,94]

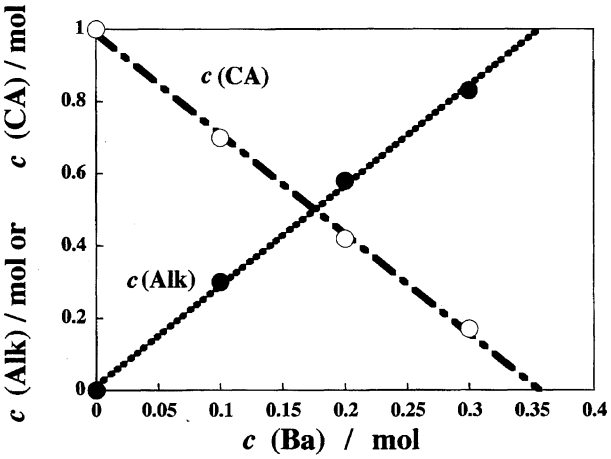

Fig. 14. Plots of c(Alk) and c(CA) against c(Ba) for solutions with the molar ratio Ba : Ti : CA : EG = 0 : 0 : 1 : 4, 0.1 : 0.1 : 1 : 4, 0.2 : 0.2 : 1 : 4, and 0.3 : 0.3 : 1 : 4. For definition of c(Alk), c(CA), and c(Ba), see text.[94]

The heterometallic BaTi–CA_n complex was isolated as a crystal with the chemical formula of $BaTi(C_6H_6O_7)_3 \cdot 4H_2O$, the composition of which was determined by a standard ICP (Inductively Coupled Plasma) and elemental analysis.[94] A number of spectroscopic characterizations have then been performed for this compound in order to gain insight into the coordination structure.

Figure 15 shows a selected region of a Raman spectrum of $BaTi(C_6H_6O_7)_3 \cdot 4H_2O$, which is compared with those of pure anhydrous CA and a CA/EG solution containing both Ba and Ti with a molar ratio of Ba : Ti : CA : EG = 0.3 : 0.3 : 1 : 4.[94] A characteristic doublet at 580 and 630 cm^{-1} (Fig. 15(b)) can be assigned, respectively, to the symmetric and antisymmetric Ti–O stretching vibrations.[97] Owing to the large mass difference between Ti and Ba, another characteristic feature showing up as a strong doublet at 260 and 330 cm^{-1} upon the complexation (Fig. 15(b)) can be assigned to stretching vibrations associated with Ba–O bonds. These two characteristic doublets are similarly observed in the Raman spectrum of the solution (Fig. 15(c)), suggesting that the basic environment around the Ba–O and Ti–O bonds in the heterometallic complex is preserved also in solutions.

The –C=O (in –COOH) or –C–O^- (in –COO^-) bonding region with a vibrational feature occurring in the range of 1500—1800 cm^{-1} is of particular importance, as the frequency may provide information on the bonding fashion of –COOH (or –COO^-) towards metal ions. Figure 16 com-

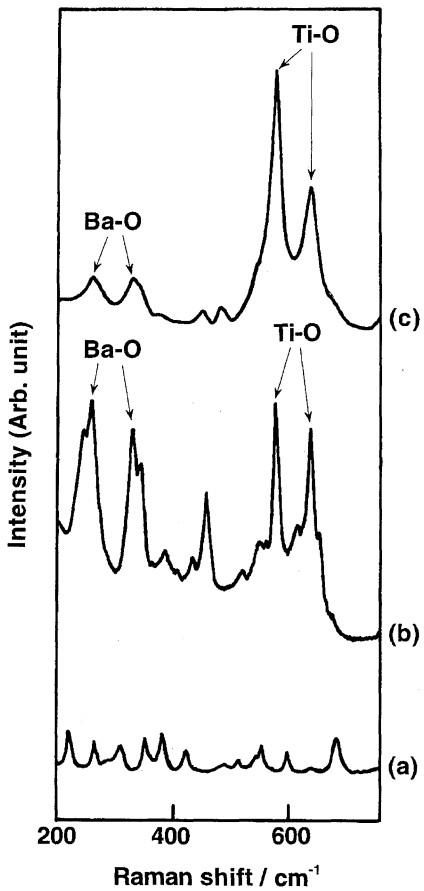

Fig. 15. Raman spectra in a region of 200—780 cm^{-1} for (a) anhydrous citric acid, (b) $BaTi(C_6H_6O_7)_3 \cdot 4H_2O$, and (c) a solution with the molar ratio Ba : Ti : CA : EG = 0.3 : 0.3 : 1 : 4. Symbols of Ti–O and Ba–O stand for stretching vibrations between oxygen and each metal.[94]

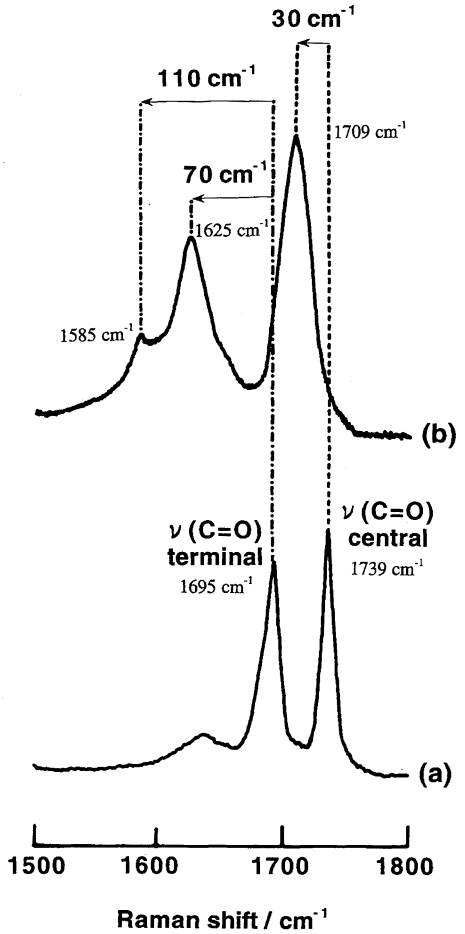

Fig. 16. Raman spectra in a region of 1500—1800 cm^{-1} for (a) anhydrous citric acid and (b) $BaTi(C_6H_6O_7)_3 \cdot 4H_2O$.[94] "$\nu$(C=O) terminal" and "$\nu$(C=O) central" denote terminal and central carboxyl C=O stretching modes in CA, respectively. Wavenumbers with arrows indicate magnitude of shifts upon complexation.

pares a Raman spectrum of $BaTi(C_6H_6O_7)_3 \cdot 4H_2O$ with that of anhydrous CA for a frequency region of 1500—1800 cm^{-1}.[94] The two rather strong and sharp peaks at 1739 and 1695 cm^{-1} in anhydrous CA (Fig. 16(a)) can be, respectively, assigned to the central carboxyl ν(C=O) stretching and the terminal carboxyl ν(C=O) stretching modes,[96] and they are used as a guide for knowing whether or not –COOH in CA is coordinated to metals. A relatively broad feature around 1630 cm^{-1} in Fig. 16(a) is attributable to the stretching vibration associated with another terminal carboxyl C=O bond with a strong intramolecular hydrogen bond,[96] and therefore it is not suitable for the use as a guide for knowing the coordination behavior of –COOH. The reference terminal carboxyl ν(C=O) mode at 1695 cm^{-1} in pure CA has splitted into two peaks at 1625 and 1585 cm^{-1} upon complexation. The observed large shifts of 70 and 110 cm^{-1} suggest that the two terminal COOH groups in CA coordinate to either Ti^{4+} or Ba^{2+}. It is plausible that the 1585 cm^{-1} peak is associated with coordination of CA to Ti, since the largest shift of 110 cm^{-1} of this mode suggests that it coordinates to Ti^{4+} with a higher valency (rather than Ba^{2+} with a lower valency) to form a stronger bond between Ti^{4+} and O, thus weakening the bond strength between carbon and oxygen atoms. The peak at 1625 cm^{-1} has an intensity much stronger than that of the peak at 1585 cm^{-1}. This may indicate that the 1625 cm^{-1} peak corresponds to C=O stretch in one of the two terminal –COOH groups in CA and the 1585 cm^{-1} peak to antisymmetric –COO stretch in carboxylate $–COO^-$, as a result of dissociation of one proton from another terminal –COOH. The basis for this interpretation has come from the generally accepted rule that bands associated with the carboxylate C–O stretch in $–COO^-$ groups have relatively low intensity in the Raman spectrum, while bands associated with carbonyl C=O stretch in –COOH groups have high intensity in the Raman spectrum.[96,102] In contrast to the behavior of the terminal COOH groups, the central carboxyl ν(C=O) mode has shifted only 30 cm^{-1} from 1739 to 1709 cm^{-1} upon the formation of $BaTi(C_6H_6O_7)_3 \cdot 4H_2O$, suggesting that the central carboxyl C=O does not coordinate to any metals. In view of these considerations, we propose that one of the two terminal COOH groups of each CA in $BaTi(C_6H_6O_7)_3 \cdot 4H_2O$ coordinates to Ba, another terminal COOH group of each CA dissociates one proton to form $–COO^-$, which coordinates to Ti in a monodentate fashion, and finally the central COOH group of each CA is not coordinating.

A selected region of solid-state ^{13}C NMR spectra of anhydrous CA and $BaTi(C_6H_6O_7)_3 \cdot 4H_2O$ is shown in Figs. 17(a) and 17(b), respectively.[94] An inspection of the alcoholic carbon region for the spectrum of $BaTi(C_6H_6O_7)_3 \cdot 4H_2O$ shows the complete absence of the resonance at 73 ppm characteristic for the alcoholic carbon in pure CA, instead of which a new triplet shows up in the region of 90 ppm. This observation, in agreement with our conclusion derived from the solution-state ^{13}C NMR spectroscopy, indicates that the alcohol OH in CA is fully deprotonated to form an alkoxide oxygen atom. The magnetic environment for each of alkoxide carbons in the three coordinating CA slightly differs from each other, which leads to the observation of the triplet at ca. 90 ppm.

A possible model for the coordination structure in the BaTi–CA_3 complex inferred from the spectroscopic data mentioned above was then proposed; shown in Fig. 18 is our proposed model for the structure of $BaTi(C_6H_6O_7)_3$, in which positions of each atom have been optimized by a Molecular Mechanics calculation.[94] It displays six-coordinated titanium and barium centers. The salient feature of the CA ligand is its tridentate nature as a whole molecule. Ba and Ti atoms are bridged by one alkoxide oxygen atom of the fully deprotonated CA ligand, and such an alkoxide oxygen atom together with two terminal carboxyl C=O groups builds up a fused 6-membered chelate ring.

(4.2.3) Improved Homogeneity by Confinement of BaTi–CA_3 in Polymer. It is important to know the thermal stability of BaTi–CA_3 during polymerization, since decomposition of the complex at an early stage of the polymerization may result in segregation of the constituent metals, thus leading to local inhomogeneity in the resulting resin. It is ^{13}C NMR and Raman spectroscopy that can be used as a

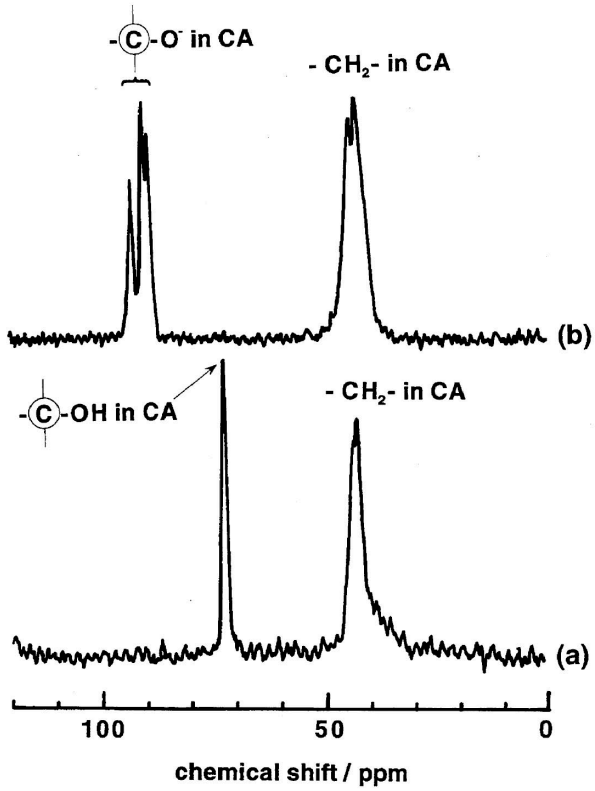

Fig. 17. Solid-state ^{13}C NMR spectra in a region of 0—120 ppm of (a) anhydrous citric acid and (b) BaTi-$(C_6H_6O_7)_3 \cdot 4H_2O$. Tetramethylsilane (TMS) was used as a reference for reported ^{13}C chemical shifts.[94]

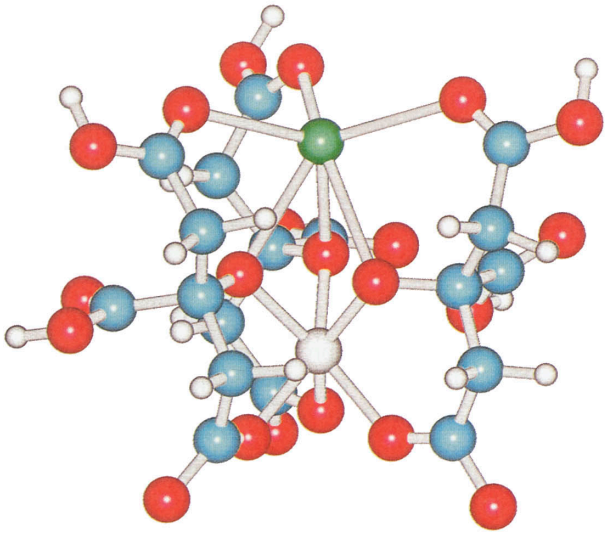

Fig. 18. A proposed model for the structure of BaTi-$(C_6H_6O_7)_3$ species.[94] Ba and Ti atoms positioned at centers are depicted by large spheres colored, respectively, in green and gray. C, O, and H atoms in citric acid are depicted by sky blue, red and small gray spheres, respectively.

convenient means for knowing such decomposition, if any.[27]

Figure 19 shows ^{13}C NMR spectra for the initial (Ba, Ti)–CA/EG solution and solutions after reactions at 135 °C for 0.5 or 1 h.[27] The fact that the intensities of the key peak at 91 ppm (attributable to the alkoxylato–CA in BaTi–CA_3) rel-

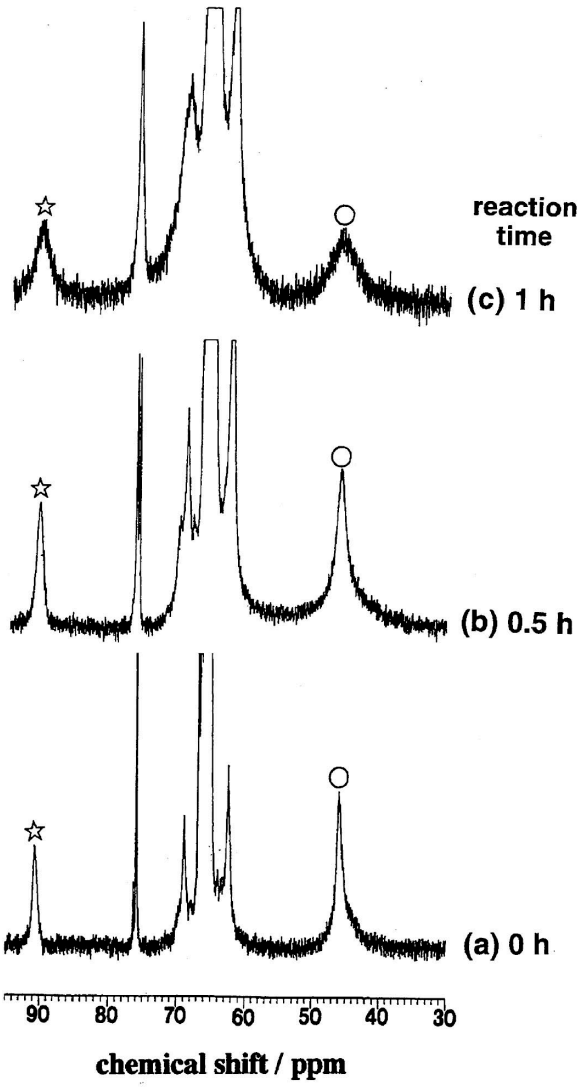

Fig. 19. ^{13}C NMR spectra of (BaTi)–CA/EG solutions reacted at 135 °C for (a) 0, (b) 0.5, and (c) 1 h. Ba : Ti : CA : EG = 0.2 : 0.2 : 1 : 4.[27] Observed broadening with increasing reaction time comes from increased viscosity of the solution.

ative to those of methylene carbon in CA at 46 ppm (marked with ○) remain almost unchanged throughout the reaction at 135 °C suggests the high thermal stability of BaTi–CA_3. Samples prepared by reactions of long duration became too viscous for their ^{13}C NMR spectra to be measured, because of the pronounced line broadening of the spectra. For such viscous samples, FT-Raman spectroscopic measurements were carried out. Figure 20 shows the ν(Ti–O) region of FT-Raman spectra of a series of (Ba/Ti)–CA/EG samples; these were prepared by reacting the initial solution at 135 °C for different duration ranging from 0 to 23 h.[27] The viscosity of the starting solution at 135 °C was below 0.1 P, while those of the remaining solutions were 0.2, 7, and 110 P, respectively. The last sample with the highest viscosity took resin form at room temperature. The characteristic Raman band at 580 cm^{-1}, which was assigned to Ti–O vibrations in BaTi–CA_3,[27,94] was observed without any noticeable change

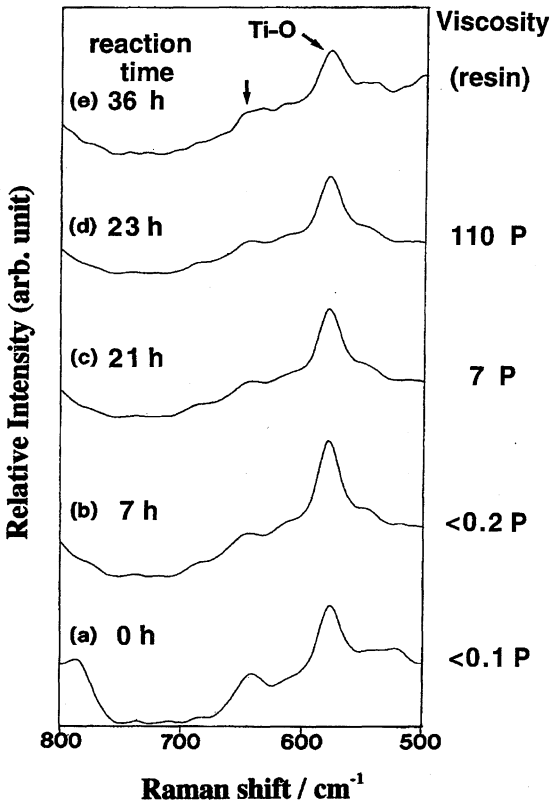

Fig. 20. FT-Raman spectra of (BaTi)–CA/EG solutions reacted at 135 °C for different durations (0—36 h). Viscosity of each solution at 135 °C is (a) <0.1 P, (b) < 0.2 P, (c) 7 P, and (d) 110 P; the last sample (e) is completely of resin. Ba : Ti : CA : EG = 0.2 : 0.2 : 1 : 4.[27]

in its position for all the solutions tested, even after the solution became completely of resin as a result of a prolonged reaction at 135 °C for up to 36 h (Fig. 20(e)). This strongly suggests that BaTi–CA_3 is thermally stable upon polymerization at 135 °C and that the basic coordination structure remains unchanged in the polymeric resin. It is tempting to state here that the formation of a stable BaTi–CA_3 complex and the maintenance of its atomic scale mixing during the course of polymerization would be one of the most important factors for achieving complete atomic mixing of barium and titanium in the pyrolyzed product. Thermolysis of the pyrolyzed products at 500 °C in static air gave pure $BaTiO_3$. It was then proposed that homogeneity at the molecular level may be responsible for the low crystallization temperature of $BaTiO_3$.[27,94]

5. Comparison with "Polymer Complex Solution (PCS)" Method

The Pechini-type **IPC** method is quite attractive in that this method can yield homogeneous oxides even when the composition is very complicated. However, the technique generally suffers from its own unique problems such as effective removal of large amounts of organics, a tendency to form hard agglomerates during the calcination of the resin and large shrinkage during heat treatment. The last disadvantage renders fabrication of fibers or films by this technique rather difficult. This explains why most of the previously reported works employing organic polymeric resin routes have been confined to powder synthesis with a few exceptions.[23,31,103—109] The polymer complex solution (**PCS**) method may overcome some of these problems, while keeping its unique advantage of the **IPC** processing. Indeed, the **PCS** technique has been successfully applied to the synthesis of high-T_c superconducting oxides with very complicated compositions.[10]

The **PCS** route is a simple "gel" related method, which is basically similar to the Pechini-type **IPC** method. In most of the **PCS** routes, the first step is to prepare an aqueous precursor solution containing metal salts, followed by addition of a water-soluble polymer. The water-soluble polymers most commonly used in the **PCS** route involve polyvinyl alcohol (PVA), polyacrylic acid (PAA), and polyethyleneimine (PEI), since they are organic polymers coordinating to cations. The basic idea behind the **PCS** route is to lower the mobility of free metal ions in a polymer solution by increasing interaction between metals and polymers. Removal of the excess water forces the polymer species into closer proximity, which increases the probability of crosslinking between them. Metal ions often behave as cross-linking centers between polymers when the polymer possesses the ability to form metal–polymer complexes. Random crosslinking across polymer chains would entrap waters in growing three-dimensional networks, which can convert the system into a "gel." Immobilization of cations in highly crosslinked polymers is thought to imply inhibition of segregation of metal ions throughout the resulting gel.

Gulgun et al.[110] have indicated in the synthesis of calcium aluminate powders from the Pechini-type **IPC** method that the polymeric resin is able to accommodate a higher amount of cations than it can chelate in the solution. Subsequently, Gulgun and Kriven[111] have prepared a "gel" containing Ca and Al ions starting from an aqueous PVA precursor without forming precipitation, and have demonstrated that the PVA-based **PCS** process requires a considerably smaller amount of organics, when compared with the Pechini-type **IPC** method.

We have also demonstrated[112] in the PVA-based **PCS** synthesis of ZrO_2–12 mol% CeO_2 that the total weight of organics required for producing one gram of ceramics is reduced by a factor of about 20 when compared with the ordinary Pechini-type **IPC** processing for the same type of materials.[57] Samples of ZrO_2-12 mol% CeO_2 were prepared by the PVA-based **PCS** method according to the flow chart of Fig. 21.[112] All the decomposition products of the polymer "gel" at 400—800 °C gave reflection peaks indexed by the fluorite-type cubic structure without any indication of impurities (Fig. 22).[112] These samples showed Raman spectra characteristic of the tetragonal zirconia, even for the sample heated at 400 °C.[112] Thus, these samples heated up to 400 °C and 800 °C are tetragonal phase whose crystalline size is too small to detect the difference between the *a*- and *c*-axes owing to the line broadening. Note also that the PVA-based **PCS** technique produces phase pure $Zr_{0.88}Ce_{0.12}O_2$ at reduced temperatures (400—800 °C),[112] as opposed to the conventional solid-state reaction methods in which process-

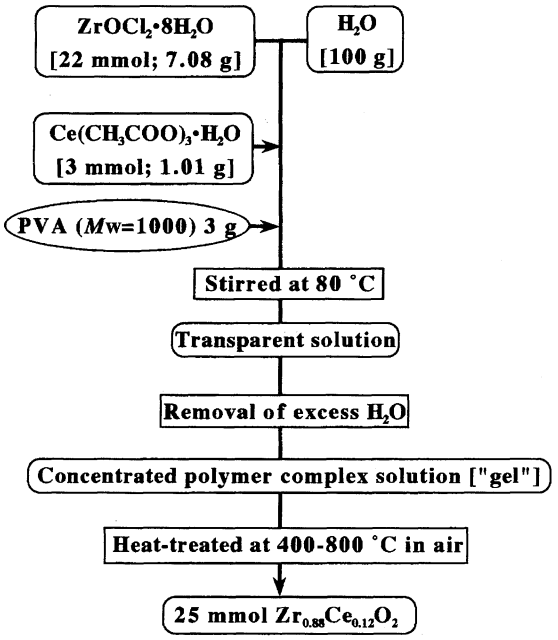

Fig. 21. Flow chart for preparing $Zr_{0.88}Ce_{0.12}O_2$ by the PVA-based **PCS** method.[112] Molecular weight of PVA used is 1000.

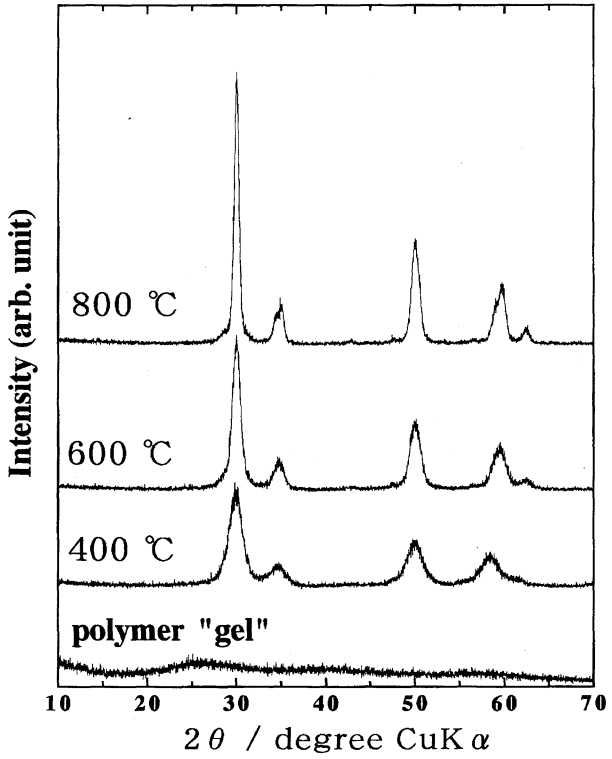

Fig. 22. X-Ray diffraction patterns of products obtained by calcining the PVA-based **PCS**-derived powder precursor for $Zr_{0.88}Ce_{0.12}O_2$.[112]

ing temperatures higher than 1400 °C are usually required for a single-phase material.[113—115] The success in lowering the crystallization temperature down to 400—800 °C again indicates an improved level of mixing of cations in the precursors.

6. Concluding Remarks

A key advantage of the Pechini-type **IPC** method over other methods is its ability to yield multicomponent oxide powders with an exceptionally good homogeneity. In particular, utilization of heterometallic complexes in the Pechini-type **IPC** processing would be one of the most promising approaches to achieve an ultimate level of homogeneity with respect to distribution of metals. Spectroscopies such as ^{13}C NMR and Raman scattering play a major role in elucidating the coordination structure of such heterometallic complexes in solutions. One of the most serious obstacles that prevents further progress of the Pechini-type **IPC** method towards its industrialization is that the process requires large amounts of organics. From this viewpoint, the aqueous solution-based **PCS** method is quite attractive, since it avoids the use of organic solvents, which is of a practical advantage, and since it requires only a small amount of polymers. At present, however, the **PCS** method is confined to aqueous solution systems in which water-soluble metal salts are available. For this reason, the method is not applicable to many useful electroceramic materials including Ti, Nb, and Ta, since organic compounds of these metals are usually insoluble in water. In order to fully exploit the **PCS** method in the field of ceramics, discovery and design of water-soluble Ti, Nb, and Ta compounds are indispensable, and a close intercommunication is required between ceramic materials science and different areas of chemistry such as aqueous-solution chemistry, inorganic/organic coordination chemistry, physical chemistry based upon a variety of spectroscopies and computational chemistry.

We are grateful to a referee for his/her extremely valuable comment and critical reading of the manuscript. We wish to thank all of the co-authors whose names appear in the cited references for their skillful experiments and valuable discussions. Financial support by "Research for the Future" Program No. JSPS-RFTF96R06901 from The Japan Society for the Promotion of Science is greatly acknowledged.

References

1 B. J. J. Zelinski and D. R. Uhlmann, *J. Phys. Chem. Solids*, **45**, 1069 (1984).
2 W. J. Dawson, *Ceram. Bull.*, **67**, 1673 (1988).
3 Ph. Colomban, *Ceram. Int.*, **15**, 23 (1989).
4 L. M. Sheppard, *Am. Ceram. Soc. Bull.*, **68**, 979 (1989).
5 L. L. Hench and J. K. West, *Chem. Rev.*, **90**, 33 (1990).
6 G. L. Messing, S. C. Zhang, and G. V. Jayanthi, *J. Am. Ceram. Soc.*, **76**, 2707 (1993).
7 C. D. Chandler, C. Roger, and M. J. Hampden-Smith, *Chem. Rev.*, **93**, 1205 (1993).
8 C. N. R. Rao, R. Nagarajan, and R. Vijayaraghavan, *Supercond. Sci. Technol.*, **6**, 1 (1993).
9 Y. G. Metlin and Y. D. Tretyakov, *J. Mater. Chem.*, **4**, 1659 (1994).
10 M. Kakihana, *J. Sol–Gel Sci. Technol.*, **6**, 7 (1996).
11 D. Segal, *J. Mater. Chem.*, **7**, 1297 (1997).

12 C. Marcilly, P. Courty, and B. Delmon, *J. Am. Ceram. Soc.*, **53**, 56 (1970).
13 M. P. Pechini, U.S. Patent No. 3330697, July (1967).
14 N. G. Eror and H. U. Anderson, in "Better Ceramics Through Chemistry II," ed by C. J. Brinker, D. E. Clark, and D. R. Ulrich, *Mater. Res. Soc. Proc.*, **73**, 571 (1986).
15 H. U. Anderson, M. J. Pennell, and J. P. Guha, in "Advances in Ceramics: Ceramic Powder Science," Vol. 21, ed by G.L. Messing, K.S. Mazdiyasni, J.W. McCauley, and R.A. Harber, Am. Ceram. Soc., Westerville, OH (1987), p. 91.
16 P. A. Lessing, *Am. Ceram. Soc. Bull.*, **168**, 1002 (1989).
17 K. D. Budd and D. A. Payne, in "Better Ceramics Through Chemistry I," *Mater. Res. Soc. Sym. Proc.*, ed by C. U. Brinker, D. E. Clark, and D. R. Ulrich, Elsevier, Pittsburgh, PA (1984), Vol. 32, p. 239.
18 S. G. Cho, P. F. Johnson, and R. A Condrate, Jr., *J. Mater. Sci.*, **25**, 4738 (1990).
19 S. L. Peschke, M. Ciftcioglu, D. H. Doughty, and J. A. Voigt, *Mater. Res. Soc. Symp. Proc.*, **271**, 1011 (1992).
20 E. R. Leite, C. M. G. Sousa, E. Longo, and J. A. Varela, *Ceram. Int.*, **21**, 143 (1995).
21 E. R. Leite, J. A. Varela, E. Longo, and C. A. Paskocimas, *Ceram. Int.*, **21**, 153 (1995).
22 M. Kakihana, T. Okubo, Y. Nakamura, M. Yashima, and M. Yoshimura, *J. Sol–Gel Sci. Technol.*, **12**, 95 (1998).
23 S. Kumar and G. L Messing, *Mater. Res. Soc. Symp. Proc.*, **271**, 95 (1992).
24 S. Kumar, G. L. Messing, and W. White, *J. Am. Ceram. Soc.*, **76**, 617 (1993).
25 S. Kumar and G. L. Messing, *J. Am. Ceram. Soc.*, **77**, 2940 (1994).
26 M. Arima, M. Kakihana, M. Yashima, and M. Yoshimura, *Eur. J. Solid State Inorg. Chem.*, **32**, 863 (1995).
27 M. Arima, M. Kakihana, Y. Nakamura, M. Yashima, and M. Yoshimura, *J. Am. Ceram. Soc.*, **79**, 2847 (1996).
28 M. Kakihana, T. Okubo, M. Arima, O. Uchiyama, M. Yashima, M. Yoshimura, and Y. Nakamura, *Chem. Mater.*, **9**, 451 (1997).
29 M. Kakihana, M. M. Milanova, M. Arima, T. Okubo, M. Yashima, and M. Yoshimura, *J. Am. Ceram. Soc.*, **79**, 1673 (1996).
30 M. M. Milanova, M. Kakihana, M. Arima, M. Yashima, and M. Yoshimura, *J. Alloys Compounds*, **242**, 6 (1996).
31 S. C. Zhang, G. L. Messing, W. Huebner, and M.M. Coleman, *J. Mater. Res.*, **5**, 1806 (1990).
32 H. H. Wang, K. D. Carllson, U. Geiser, R. J. Thorn, H-C. Kao, M. A. Beno, M. R. Monaghan, T. J. Allen, R. B. Proksch, D. L. Stupka, J. M. Williams, B. K. Flandermeyer, and R. B. Poeppel, *Inorg. Chem.*, **26**, 1476 (1987).
33 S. E. Trolier, S. D. Atkinson, P. A. Fuierer, J. H. Adair, and R. E. Newnham, *Am. Ceram. Soc. Bull.*, **67**, 759 (1988).
34 H. K. Lee, D. Kim, and S. I. Suck, *J. Appl. Phys.*, **65**, 2563 (1989).
35 H. K. Lee, K. W. Lee, D. H. Ha, K. Park, and J. C. Park, *Appl. Phys. Lett.*, **55**, 1249 (1989).
36 W. J. Thomson, H. Wang, D. V. Parkman, D. X. Li, M. Strasik, T. S. Luhman, C. Han and I. A. Aksay, *J. Am. Ceram. Soc.*, **72**, 1977 (1989).
37 G. Paz-Pujalt, *Physica C*, **166**, 177 (1990).
38 L. Ben-Dor, H. Diab, and I. Felner, *J. Solid State Chem.*, **88**, 183 (1990).
39 M. Kakihana, L. Borjesson, S. Eriksson, and P. Svedlindh, *J. Appl. Phys.*, **69**, 867 (1991).
40 M. Kakihana, M. Kall, L. Borjesson, H. Mazaki, H. Yasuoka, P. Berastegui, S. Eriksson, and L-G. Johansson, *Physica C*, **173**, 377 (1991).
41 T-M. Chen and Y. H. Hu, *Physica C*, **190**, 124 (1991).
42 H. Mazaki, M. Kakihana, and H. Yasuoka, *Jpn. J. Appl. Phys.*, **30**, 38 (1991).
43 M. K. Agarwala, D. L. Bourell, and C. Persad, *J. Am. Ceram. Soc.*, **75**, 1975 (1992).
44 S. H. Shieh and W. J. Thomson, *Physica C*, **204**, 135 (1992).
45 T-M. Chen and Y. H. Hu, *J. Solid State Chem.*, **97**, 124 (1992).
46 M. Kakihana, M. Yoshimura, H. Mazaki, H. Yasuoka, and L. Borjesson, *J. Appl. Phys.*, **71**, 3904 (1992).
47 R. Mahesh, R. Nagarajan, and C. N. R. Rao, *J. Solid State Chem.*, **96**, 2 (1992).
48 P. Berastegui, M. Kakihana, M. Yoshimura, H. Mazaki, H. Yasuoka, L-G. Johansson, S. Eriksson, L. Borjesson, and M. Kall, *J. Appl. Phys.*, **73**, 2424 (1993).
49 H. Mazaki, H. Yasuoka, M. Kakihana, H. Fujimori, M. Yashima, and M. Yoshimura, *Physica C*, **246**, 37 (1995).
50 M. Kakihana, M. Arima, M. Yoshimura, N. Ikeda, and Y. Sugitani, *J. Alloys Compounds*, **283**, 102 (1999).
51 M. Kakihana and T. Okubo, *J. Alloys Compounds*, **266**, 129 (1998).
52 L.W. Tai and P.A. Lessing, *J. Mater. Res.*, **7**, 511 (1992).
53 T. Okubo and M. Kakihana, *J. Alloys Compounds*, **256**, 151 (1997).
54 J. Szanics, T. Okubo, and M. Kakihana, *J. Alloys Compounds*, **281**, 206 (1999).
55 S. Ikeda, M. Hara, J. N. Kondo, K. Domen, H. Takahashi, T. Okubo, and M. Kakihana, *Chem. Mater.*, **10**, 72 (1998).
56 S. Ikeda, M. Hara, J. N. Kondo, K. Domen, H. Takahashi, T. Okubo, and M. Kakihana, *J. Mater. Res.*, **13**, 852 (1998).
57 M. Yashima, K. Ohtake, M. Kakihana, and M. Yoshimura, *J. Am. Ceram. Soc.*, **77**, 2773 (1994).
58 O. Yokota, M. Yashima, M. Kakihana, A. Shimofuku, and M. Yoshimura, *J. Am. Ceram. Soc.*, **82**, 1333 (1999).
59 J. Ma, M. Yoshimura, M. Kakihana, and M. Yashima, *J. Mater. Res.*, **13**, 939 (1998).
60 M. Yoshimura, J. Ma, and M. Kakihana, *J. Am. Ceram. Soc.*, **81**, 2721 (1998).
61 C. O. Udawatte, M. Kakihana, and M. Yoshimura, *Solid State Ionics*, **108**, 23 (1998).
62 M. Kakihana, M. Arima, T. Sato, K. Yoshida, Y. Yamashita, M. Yashima, and M. Yoshimura, *Appl. Phys. Lett.*, **69**, 2053 (1996).
63 Y. Yamashita, K. Yoshida, M. Kakihana, S. Uchida, and T. Sato, *Chem. Mater.*, **11**, 61 (1999).
64 H. Takahashi, M. Kakihana, Y. Yamashita, K. Yoshida, S. Ikeda, M. Hara, and K. Domen, *J. Alloys Compounds*, **285**, 77 (1999).
65 T. Furukawa and W. B. White, *Phys. Chem. Glasses*, **20**, 69 (1979).
66 U. Balachandran and N. G. Eror, *J. Solid State Chem.*, **42**, 276 (1982).
67 J. J. Ritter, R. S. Roth, and J. E. Blendell, *J. Am. Ceram. Soc.*, **69**, 155 (1986).
68 J. Livage, M. Henry, and C. Sanchez, *Prog. Solid State Chem.*, **18**, 259 (1988).
69 S. Doeuff, M. Henry, C. Sanchez, and J. Livage, *J. Non-Cryst. Solids*, **89**, 206 (1987).
70 C. Sanchez, J. Livage, M. Henry, and F. Babonneau, *J. Non-Cryst. Solids*, **100**, 65 (1988).

71 J. H. Choy, Y. S. Han, J. T. Kim, and Y. H. Kim, *J. Mater. Chem.*, **5**, 57 (1995).

72 P. P. Phule and S. H. Risbud, "Better Ceramics through Chemistry III," ed by C. J. Brinker, D. E. Clark, and D. R. Ulrich; *Mater. Res. Soc. Symp. Proc.*, **121**, 275 (1988).

73 M. Kakihana, M. Arima, M. Yashima, M. Yoshimura, Y. Nakamura, H. Mazaki, and H. Yasuoka, in "Sol–Gel Science and Technology," ed by E. J. A. Pope, S. Sakka, and L. C. Klein, Ceramic Transactions, Am. Ceram. Soc., Westerville, OH, **55**, 65 (1995).

74 Y. Inoue, T. Kubokawa, and K. Sato, *J. Chem. Soc., Chem. Commun.*, **1990**, 1298.

75 Y. Inoue, T. Kubokawa, and K. Sato, *J. Phys. Chem.*, **95**, 4095 (1991).

76 Y. Inoue, T. Niiyama, Y. Asai, and K. Sato, *J. Chem. Soc., Chem. Commun.*, **1992**, 579.

77 Y. Inoue, Y. Asai, and K. Sato, *J. Chem. Soc., Faraday Trans.*, **90**, 797 (1994).

78 M. Kohno, S. Ogura, and Y. Inoue, *J. Mater. Chem.*, **6**, 1921 (1996).

79 K. G. Caulton and L. G. Hubert-Pfalzgraf, *Chem. Rev.*, **90**, 969 (1990).

80 R. C. Mehrotra, *Mater. Res. Soc. Symp. Proc.*, **121**, 81 (1988).

81 R. C. Mehrotra, M. M. Agarwal, and P. N. Kapoor, *J. Chem. Soc. A*, **1968**, 2673.

82 D. J. Eichorst, K. E. Howard, and D. A. Payne, in "Ultrastructure Processing of Advanced Materials," ed by D. R. Uhlmann and D. R. Ulrich, J. Wiley & Sons, New York (1992), Chap. 8.

83 D. J. Eichorst, D. A. Payne, and S. R. Wilson, *Inorg. Chem.*, **29**, 1458 (1990).

84 R. S. Weis and T. K. Gaylord, *Appl. Phys. A*, **37**, 191 (1985).

85 D. J. Eichorst and D. A. Payne, *Mater. Res. Soc. Symp. Proc.*, **121**, 773 (1988).

86 S. Hirano and K. Kato, *J. Non-Cryst. Solids*, **100**, 538 (1988).

87 S. Hirano, T. Yogo, and K. Kikuta, *J. Ceram. Soc. Jpn.*, **99**, 1026 (1991).

88 S. Hirano, T. Yogo, K. Kikuta, H. Urahata, Y. Isobe, T. Morishita, K. Ogiso, and Y. Ito, *Mater. Res. Soc. Symp. Proc.*, **271**, 331 (1992).

89 D. J. Eichorst, D. A. Payne, and A. N. A. Wragg, in "Ceramic Thick and Tnin Films," ed by B. Hiremath, Am. Ceram. Soc., p. 375 (1990).

90 D. C. Bradley, R. C. Mehrotra, and D. P. Gaur, "Metal Alkoxides," Academic Press, London (1978).

91 J. F. Campion, J. K. Maurin, D. A. Payne, and S. R. Wilson, *Inorg. Chem.*, **30**, 3244 (1991).

92 Z. Xu, H. K. Chae, M. H. Frey, and D. A. Payne, *Mater. Res. Soc. Symp. Proc.*, **271**, 339 (1992).

93 A. J. Moulson and J. M. Herbert, "Electroceramics: Materials, Properties and Applications," Chapman and Hall, London (1990).

94 M. Kakihana, M. Arima, Y. Nakamura, M. Yashima, and M. Yoshimura, *Chem. Mater.*, **11**, 438 (1999).

95 L. J. Bellamy, "The Infra-red Spectra of Complex Molecules," Chapman and Hall, London, U. K. (1975), pp. 176—179.

96 P. Tarakeshwar and S. Manogran, *Spectrochim. Acta*, **50A**, 2327 (1994).

97 M. J. Payne and K. A. Berglund, *Mater. Res. Soc. Symp. Proc.*, **73**, 571 (1986).

98 L. F. Johnson and W.C. Jankowski, " ^{13}C- NMR Spectra," John Wiley & Sons, Inc., New York (1972).

99 T. Fujita, *Chem. Pharm. Bull.*, **30**, 3461 (1982).

100 J. Strouse, S. W. Layten, and C. E. Strouse, *J. Am. Chem. Soc.*, **99**, 562 (1977).

101 N. N. Tananaeva, E. K. Trunova, N. A. Kostromina, and Yu. B. Shevchenko, *Teor. Eksp. Khim.*, **26**, 706 (1990).

102 K. Nakamoto, "Infrared and Raman Spectra of Inorganic and Coordinate Compounds," 4th ed, Wiley, New York (1986).

103 Y-M. Chiang, S. L. Furcone, J. A. S. Ikeda, and D. A. Rudman, *Mater. Res. Soc. Symp. Proc.*, **99**, 307 (1988).

104 J. McKittrick and R. Contreras, *Thin Solid Films*, **206**, 146 (1991).

105 T. W. Kueper, S. J. Visco, and L. C. DeJonghe, *Solid State Ionics*, **52**, 251 (1992).

106 C. C. Chen, M. M. Nasrallah, and H. U. Anderson, *J. Electrochem. Soc.*, **140**, 3555 (1993).

107 M. Liu and D. Wang, *J. Mater. Res.*,**10**, 3210 (1995).

108 V. Agarwal and M. Liu, *J. Mater. Sci.*, **32**, 619 (1997).

109 V. Bouquet, E. R. Leite, E. Longo, and J. A. Varela, *Key Eng. Mater.*, **132-136**, 1143 (1997).

110 M. A. Gulgun, O. O. Popoola and W. M. Kriven, *J. Am. Ceram. Soc.*, **77**, 531 (1994).

111 M. A. Gulgun and W. M. Kriven, *Ceram. Trans.*, **62**, 57 (1996).

112 M. Kakihana, S. Yamamoto, and S. Kato, submitted to *Chem. Mater.* (1999).

113 M. Yashima, K. Morimoto, N. Ishizawa, and M. Yoshimura, *J. Am. Ceram. Soc.*, **76**, 1745 (1993).

114 M. Yashima, K. Morimoto, N. Ishizawa, and M. Yoshimura, "Science and Technology of Zirconia V," ed by S. P. S. Badwal, M. J. Bannister, and R. H. J. Hannink, Technomic Publishing Company, Lancaster, PA (1993).

115 J. Lefevre, *Ann. Chim.*, **7**, 117 (1963).

Masato Kakihana was born in 1954 in Tokyo. He received his B.S. (1978) and M.S. (1980) from Sophia University under the supervision of Prof. G. P. Sato, and Dr. of Science degree (1983) from Tokyo Institute of Technology under the supervision of Prof. M. Okamoto. From 1983 to 1991, he joined Department of Chemistry, National Defense Academy as a research associate, and in the mean time he worked as a visiting scientist for Prof. Lena Torell at Department of Physics, Chalmers University of Technology (1987—1989). In 1991 he was appointed to Associate Professor at Research Laboratory of Engineering Materials (RLEM), Tokyo Institute of Technology (TIT), and in 1996 reappointed to Associate Professor at Materials and Structures Laboratory (former RLEM), TIT. His current interest is focused on solution based-synthesis of ceramics and of application of Raman spectroscopy to inorganic materials.

Masahiro Yoshimura received B.S. in 1965, M.S. in 1967, and Dr. Sci. in Engineering in 1970 in Inorganic Materials Division,Tokyo Institute of Technology. He was a Research Associate in 1970, Associate Professor in 1978, a Professor in 1985 at Research Laboratory of Engineering Materials (name changed to Materials and Structures Laboratory in 1996), Tokyo Institute of Technology, and currently the Director of Center for Materials Design. He was visiting fellow in 3 CNRS Laboratories in France from 1973 to 1975, and in Ceramic Department, Massachusetts Institute of Technology, U.S.A., from 1975 to 1977. He is currently proposing a new concept, "Soft Solution Processing": Environmentally friendly methods for synthesis/fabricating of advanced ceramics.